

## 1

## Nanostructured Electrodes with Unique Properties for Biological and Other Applications

*J. Justin Gooding, Leo M.H. Lai, and Ian Y. Goon*

## 1.1

### Introduction

Modifying the surface of electrodes to provide some control over how the electrode interacts with its environment has been one of the most active areas of research interest in electrochemistry within the last 30 years [1]. Whereas once the performance of an electrode was limited to the solution it was placed into, the material from which the electrode was made and the potential applied to the surface, the ability to chemically modify electrodes has provided a powerful route to tuning their performance. This has been particularly important to electroanalytical chemistry [2, 3], where modification has provided routes to providing selectivity, resisting fouling, concentrating species, improving electrocatalytic properties [4] and limiting access of interferences in a complex sample [5], such as a biological fluid, but has also had major impact for research into energy conversion [6, 7] and storage, corrosion protection [8], molecular electronics [9–11], electrochromic devices [12] and fundamental research into phenomena that influence electrochemical processes [9]. In recent years this revolution into tailoring electrode surfaces, such that the electrode has unique properties, has continued at an even greater rate with unprecedented control over the modification process via advances in nanofabrication. Taken in its broadest context, nanostructuring electrodes can be regarded as controlling the architecture of an electrode at the nanoscale; whether it be using nanomaterials, templating methods, organic monolayer modification of electrode surfaces or hybrid modification layers involving organic monolayers and nanomaterials. These different strategies for modifying electrodes provide opportunities to confer a unique range of properties to electrode surfaces from ultrahigh surface areas achieved with templated electrodes, to electrocatalytic properties with nanoparticles, strategies to achieve electrochemistry in locations too small for conventional electrodes, such as inside enzymes, and give electrodes with switchable properties.

Many of the unique properties that can be achieved with nanostructuring at the nanoscale are due to the ability of the unique properties of the nanomaterials employed, the ability to control the architecture of the electrode interface at the

nanoscale or both. This nanoscale design of electrode interfaces potentially provides spatial control vertically from the surface and/or laterally across the electrode surface. In many ways self-assembled monolayers (SAMs) and templated methods offer the greatest possible control over how an electrode interface is modified as the electrode design and properties are tailored at something akin to the molecular level [13–15]. This spatial control is coupled with chemical control via the ability to incorporate multiple chemical components into a single interface to provide the interface with a range of properties. An example of such control is in the ion-channel biosensor where up to 10 or more molecular components are incorporated into a lipid bilayer for modifying electrodes where both lateral and vertical control are required to give one of the most versatile and sensitive biosensing concepts ever developed [16]. It is this molecular-level control with monolayer technologies that also forms the basis of many unique nanostructured electrode concepts involving nanoparticles, nanotubes and other nanomaterials where self-assembled monolayers form the linker between a macroscopic electrode and the nanomaterial [14].

It is the unique properties that can be conferred to an electrode by nanostructuring using nanomaterials, self-assembled monolayers and templating methods, particularly with regards to a biological context, that are the subject of this chapter. The chapter is not intended to be a comprehensive review of all the work done on nanostructuring electrodes but rather to cover some of the recent advances in nanostructuring electrodes, which are important for using electrodes for biological applications. Firstly, strategies to produce electrodes with high surface areas and their applications in enhancing electrode sensitivity will be discussed. The discussion of surface area will be followed by the structuring of electrodes with nanoscale features that provide catalytic properties to the electrode. The third section will cover the small size of features providing the opportunity to intimately interface electrodes with proteins. This section will include using molecular wires to give blocked electrodes where electrochemical communication is maintained through molecular wires. The final section of the chapter will explore switchable surfaces where spatial modulation of the electrode modification layer is exploited to radically alter the properties of the electrodes. In all cases our emphasis will be on methods of electrode modification that are highly controlled.

## 1.2 High Surface Area Electrodes

Incorporation of nanostructures onto the surface of electrodes began in the early 1990s. These structures were initially used to enhance electrochemical signals due to their high surface-to-volume ratio. Gradually, work progressed to their application into bioconjugated systems. The increase in electroactive surface area allows for lower detection limits and higher sensitivity to analytes. This is demonstrated in the detection of  $\text{H}_2\text{O}_2$  using films of nanoparticles in a three-dimensional structure [17, 18]. In these studies, multilayers of nanoparticles were built up with bridging molecules between the layers. The bridging molecules have redox-active

centers, which are sensitive to  $\text{H}_2\text{O}_2$ . By having large areas of nanoparticle film, the number of redox-active centers increases, providing a more sensitive sensor compared with electrodes of the same material that do not comprise the nanoparticle films. The main challenge in achieving a high surface area electrode is the control over the size and distribution of the structures produced on the electrode surface. To accomplish this, the four main strategies in producing high surface area electrodes that have been employed are (1) the direct attachment of nanoparticles onto an electrode, (2) templating with membranes such as polycarbonates or alumina, (3) the use of lyotropic liquid crystals as templates and (4) colloidal templating. We will discuss each of these in this section.

### 1.2.1

#### Attachment of Nanoparticles onto Electrodes

Increasing the electroactive surface area has been successfully achieved by the attachment of nanoparticles onto an electrode. Natan and coworkers [19] pioneered this approach, where the initial idea was to attach nanoparticles onto a platinum surface to enhance electrode performance. In this first study the surface of a platinum foil was coated with a polymer, (3-mercaptopropyl) methyltrimethoxysilane (MPMDMS). Subsequently, the modified electrode was placed into a solution of 15-nm diameter Au nanoparticles. The MPMDMS and Au nanoparticle-modified layer was electrochemically active to the redox-active species, methyl viologen. An important observation made by Natan and coworkers [19] in this work is the electrochemistry was blocked when the Pt foil electrode was modified with the MPMDMS in the absence of Au nanoparticles but was 'switched on' when the nanoparticles were present. This demonstrates that the Au nanoparticles act as electrodes. However, when the oxidation and reduction peaks in the cyclic voltammogram (CV) were compared to a bare platinum electrode, the peaks in the CV of the nanoparticle-modified electrode had a slight broadening. The broadening was attributed to a closely spaced array of nanoelectrodes. Although this paper did not explore the effect of multilayers of nanoparticle films, nor the enhancement of the electrochemical signal provided by the increased surface area, this work paved the way for further investigation into nanoparticle-modified electrodes in general and for sensing in particular.

Following the lead of Natan and coworkers, further studies have demonstrated the ability of nanoparticles to enhance sensitivity by constructing multilayer structures composed of nanoparticles. Multilayers of nanoparticles linked together with conductive species create large internal surface area, which can be accessible to redox probes. The multilayered systems effectively create a porous network providing much higher surface area than a monolayer. For example, Blonder *et al.* [20] have modified indium tin oxide (ITO) electrodes with multilayers of Au nanoparticles. In this example the ITO surface was first modified with triethoxy aminopropylsilane in toluene, followed by the attachment of 12-nm nanoparticles (Figure 1.1). This nanoparticle-modified layer was then further functionalized with *N,N'*-bis(2-aminoethyl)-4,4' bipyridinium, a redox-active bridging molecule. Four layers of

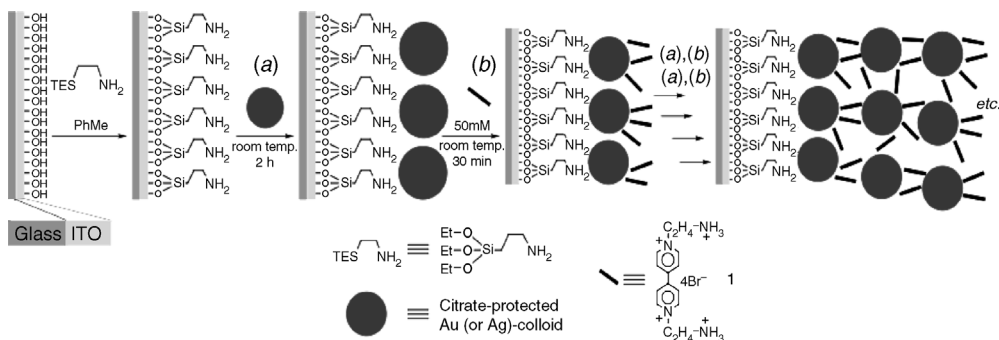


**Figure 1.1** Stepwise production of metal-particle multilayer arrays. The attachment of the Au or Ag nanoparticles onto ITO-modified glass was achieved by using silanes that have an amine terminus group. This modification step allows for further modification with nanoparticles onto the surface of the ITO. After the nanoparticle attachment a redox-active bridging molecule was assembled onto the Au or Ag nanoparticle monolayer. This step was repeated a number of times to produce a three-dimensional array of nanoparticles that has large internal surface area and increased redox-active species concentration. (Reproduced by permission of The Royal Society of Chemistry from [20].)

nanoparticle films were constructed by repeating the exposure to Au nanoparticles and the redox bridge. This study demonstrated that, as more nanoparticles were placed on the electrode, an increase in peak current was observed for the oxidation and reduction, when a cyclic voltammogram was taken in phosphate buffer at pH 7. The increase in signal was attributed to two related factors. The first was the increase in the number of redox molecules in the layer and the second was the increase in electroactive surface area.

The main idea demonstrated by Willner and coworkers [20] is the ability to construct multilayered nanoparticle electrodes, which are porous. In a related study Patolsky *et al.* extended this idea further using biocatalysts to detect  $\text{H}_2\text{O}_2$  [18]. In this example, the construction of the electrode is similar to the one described above but the redox-active bridging molecule was replaced with microperoxidase-11 (MP-11).

MP-11 is an 11 amino acid long chain, with the heme center of cytochrome *c* (Figure 1.2), which is produced by proteolytic digestion. It is an electrocatalyst and biocatalytic unit for  $\text{H}_2\text{O}_2$ . By keeping the concentration of  $\text{H}_2\text{O}_2$  constant at 0.5 mM and changing the number of layers of nanoparticles and MP-11, Willner and coworkers [18] observed the enhancement of peak current as the number of layers of nanoparticles and MP-11 deposited on the electrode was increased. Therefore, Willner and coworkers concluded that the three-dimensional structure can provide a tunable and sensitive sensing interface for  $\text{H}_2\text{O}_2$  by adjusting the amount of nanoparticle layers present in the three-dimensional structure.

Electrodeposition is an alternative way to produce nanostructures on an electrode surface from solution onto a surface. Using electrodeposition to construct nanostructures allows for greater control over the amount of material deposited on the surface due to the ability to precisely control the charge that is passed into the system. Some control over the morphology is also afforded. For example, Liu *et al.*

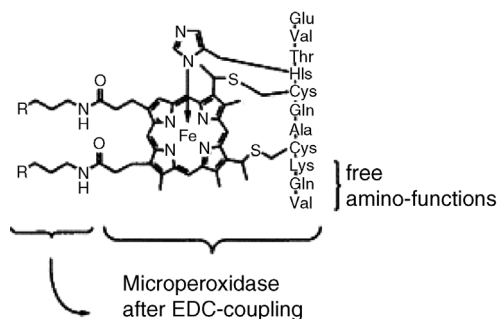


**Figure 1.2** Stepwise assembly of MP-11, Au nanoparticle superstructure on ITO. (Reprinted with permission from Ref. [18]. ©1999 Elsevier.)

demonstrated the production of pyramidal, rod-like and spherical Au structures on Au foil [21]. The production of these nanostructures was simply achieved by electrodeposition of gold from an aqueous solution of 0.1 M  $\text{HClO}_4$  and different concentrations of  $\text{HAuCl}_4$ . For example, to produce pyramidal structures 40 mM  $\text{HAuCl}_4$  was used and deposited at  $-0.08\text{ V}$  vs.  $\text{Ag}|\text{AgCl}$ , to produce rod-like structures 4 mM  $\text{HAuCl}_4$  and  $-0.08\text{ V}$  vs.  $\text{Ag}|\text{AgCl}$  was used and finally spherical structures were produced with 40 mM  $\text{HAuCl}_4$  at  $-0.2\text{ V}$  vs.  $\text{Ag}|\text{AgCl}$ . After the formation of the nanostructures the surface was modified with Cu, Zn-superoxide dismutase (Cu, Zn-SOD). The enzyme immobilization was achieved simply by adsorption. The resulting electrodes were exposed to superoxide ( $\text{O}_2^-$ ) and exhibited an improvement in the direct electron transfer between the SOD and the gold nanostructures compared with an electrode without nanostructuring. In particular the spherical nanostructured electrode showed excellent analytical performance, such as a wider linear range (0.2–200  $\mu\text{M}$ ), a lower detection limit (0.1  $\mu\text{M}$ ), a shorter response time (4.1 s) and a higher stability compared with the pyramidal and rod-like nanostructures.

The observation made by Natan and coworkers [19] that electrochemistry at a Pt foil electrode modified with the MPMDMS was dramatically altered when nanoparticles were present was also the first example where nanoparticles were used to alter the resistance of polymer films. At a similar time, Murray and coworkers [22] used nanoparticle films to explore the resistance properties of films relative to the length of the species that were used to bind the nanoparticles together into films. In this first study the modifiers were octanethiol, dodecanethiol and hexadecanethiols. The modified nanoparticles were produced by the reduction of  $\text{HAuCl}_4$  in toluene followed by extraction into toluene where a molar equivalent amount of the thiol was added. The gold nanoparticles were flocculated to give a nanoparticle film. Conductivity of the films was measured and Murray and coworkers [22] reported a significant decrease in conductivity (150 times when compared between octanethiol and hexadodecanethiol) as the length of the monolayer coating the gold nanoparticle increase. This unique ability of the dependence on length of monolayers on nanoparticle surface on resistance has been used to detect gaseous analytes.

Following the concept of Murray and coworkers, Evans *et al.* [23] applied the system to the detection of gaseous methanol, ethanol, propanol, hexane, pentane, toluene, chloroform and acetic acid samples. In this study the nanoparticles were produced by the reduction of  $\text{HAuCl}_4$  with  $\text{NaBH}_4$ . The synthesized modified nanoparticles were deposited onto an interdigitated electrode by the evaporation of the nanoparticle solution directly onto the electrode surface. The particles were tested at room temperature with no exposure to solvent vapors. Evans and coworkers observed a change in conductivity upon the change in functional groups (in decreasing order:  $\text{CH}_3 > \text{COOH} > \text{OH}$ ) and size (larger-sized nanoparticle exhibited higher conductivity). The nanoparticle films were then exposed to different solvents, both polar and nonpolar solvents. The change in conductivity with the exposure to different solvents varied depending on the functional groups. Polar groups ( $\text{OH}$ ,  $\text{NH}_2$  and  $\text{COOH}$ ) responded well to polar solvents and the nonpolar ( $\text{CH}_3$ ) group responded well to nonpolar solvents. This preliminary study demonstrated the sensitivity of different functionalized nanoparticles to different analytes, in vapor phase.

Apart from using simple molecules, alkanethiols or mercaptophenyl's more complex molecules, dendrimers have been used to modify and improve the sensing capabilities of gold nanoparticle films to vapors (Figure 1.3). In a study by Krasteva *et al.* [24] the application of dendrimers was used to functionalize, as well as linking the modified nanoparticles together to produce a conducting film of gold nanoparticles and dendrimers. The study involved three types of dendrimers, one was hydrophobic (polyphenylene: PPh), and two hydrophilic (poly-amidoamine: PAMAM and poly-propyleneimine: PPI). All the dendrimer-modified nanoparticle films were made from gold nanoparticles with an average size of 4 nm that were suspended in toluene. To construct the nanoparticle/dendrimer film a glass substrate was used, which was functionalized with aminopropyltrimethoxysilane and then placed into the gold nanoparticle solution. Then, the nanoparticle-modified glass film was placed into a solution of either PAMAM (third-generation Starburst\*) in methanol, PPI (fourth-generation DAB-Am-32-poly(propyleneimine-dotriacontamine) in methanol or PPh (second-generation dithiolane-functionlized polyphenylene) in toluene and dichloromethane. This deposition of gold nanoparticles and dendrimers was repeated ten times to ensure a full coverage on the glass surface. The dendrimer-modified nanoparticle film was then exposed to three solvents, water, 1-propanol and toluene. Depending on the dendrimer used to functionalize the nanoparticles, a change in the resistance response to different solvents was observed. The Au/PPh was the most responsive to toluene due to the nonpolar nature of both the dendrimer and solvent. Au/PPI was the most responsive to 1-propanol and Au/PAMAM was the most responsive to water. Krasteva *et al.* [24] suggested that the chemical selectivity is related to the solubility of the dendrimers to the solvent exposed. This unique ability to detect vapors of solvents by nanoparticle films modified with dendrimers, by tailoring the functionality of the molecules allows for the use in sensors.

Other materials have also been used to produce modified nanoparticle films to detect organic vapors. Murray and coworkers [26] showed that the modification of nanoparticles with a carboxylate ligand, which can complex with a metal ion,  $\text{Cu}^{2+}$ ,

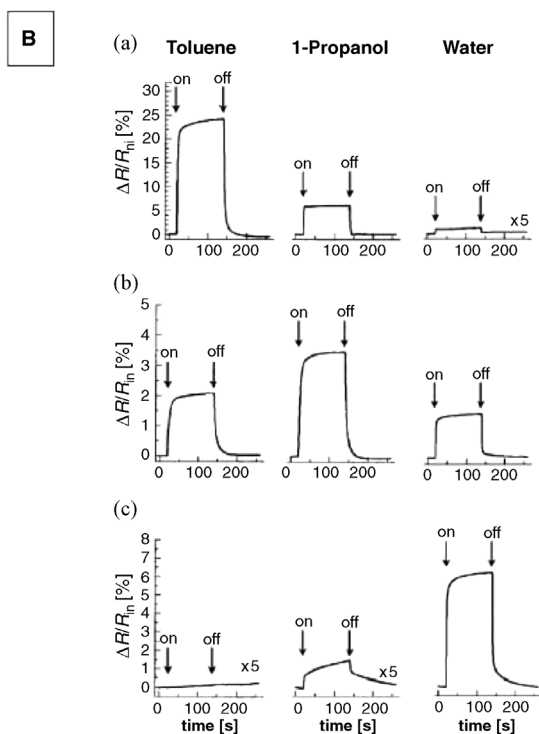
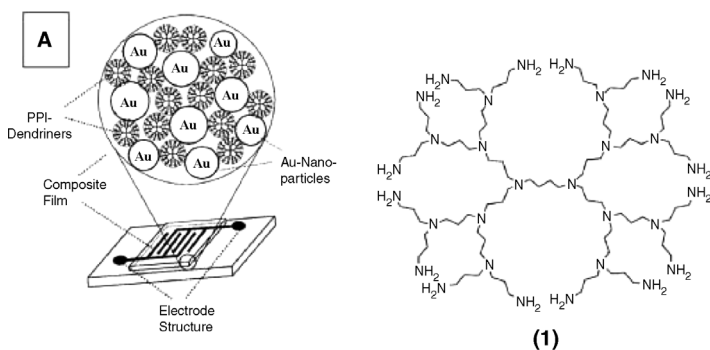


**Figure 1.3** (A) Chemresistor containing gold nanoparticles and PPI. (Reprinted with permission ©2002 American Chemical Society.) (B) Response of the Au nanoparticle film to toluene, 1-propanol and water: (a) Au/PPh; (b) Au/PPI; (c) Au/PAMAM. (Reprinted with permission ©2003 Elsevier.) (Reproduced with permission from Ref. [25] © 2004 Wiley-VCH Verlag GmbH & Co. KGaA.)

to produce a flexible network polymer film (Figure 1.4). To produce the flexible polymer film, the nanoparticles were first synthesized with a protective layer of butanethiol, hexanethiol, octanethiol, decanethiol or dodecanethiol. This initial layer acted as a capping layer rather than a linker layer. To allow the nanoparticle film to

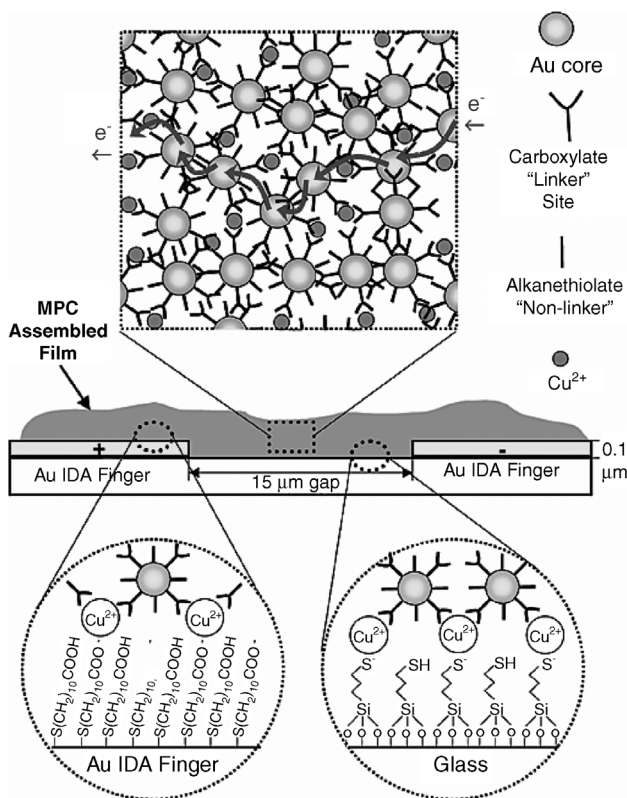


**Figure 1.4** Schematic of the flexible nanoparticle film and construction. (Reprinted with permission from Ref. [26]. ©2002 American Chemical Society.)

form, some of the capping thiols were replaced with linker molecules such as 6-mercaptohexanoic acid, 11-mercaptoundecanoic acid or 16-mercaptohexadecanoic acid, using the place-exchange reaction. To construct the nanoparticle film, firstly two gold interdigitated electrodes were modified with a layer of 11-mercaptoundecanoic acid and the glass substrate with 3-mercaptopropyltrimethoxy silane. This functionalized electrode was then exposed to  $\text{Cu}^{2+}$  ions in ethanol, which complexed with the carboxylic acid, followed by the linker-modified gold nanoparticle. After this, the nanoparticle-deposited electrodes were rinsed with ethanol and the process of exposure to  $\text{Cu}^{2+}$  and nanoparticles was repeated numerous times to construct the film over the two electrodes, which connected the two gold fingers. This film was then exposed to ethanol vapor of various concentrations (0.1–1 saturated ethanol vapor). The conductivity results were compared to quartz crystal microgravimetry (QCM) data and showed highly comparable results, where the decrease in conductivity is related to the increase in mass by the QCM data. Zamborini *et al.* [26] have also reported the rapid switching between the exposure of ethanol vapor and  $\text{N}_2$  gas. It was also reported that particles that were functionalized with 6-hexanethiol and

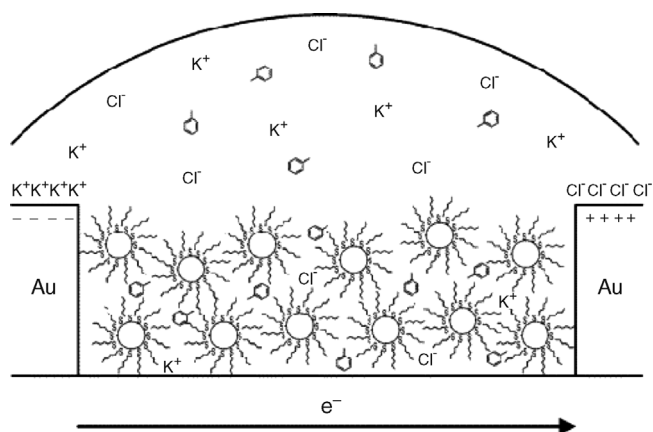


**Figure 1.5** Schematic representation of hexanethiol-modified Au nanoparticles deposited between gold electrodes, in the presence of dissolved toluene in KCl solution. (Reprinted with permission from Ref. [27] ©2007 American Chemical Society.)

11-mercaptoundecanoic acid performed the best with a fast response rate (8 s) and the highest absorption of ethanol onto the structure (68 nmol).

Many of the applications of modified nanoparticle films have been used in the detection of gaseous chemicals but have not been applied in an aqueous environment. This inability to be applied to the detection of analytes in aqueous media is due to the high conductivity of the electrolyte solution. For nanoparticle film electrodes to be able to sense in aqueous solutions, the device must be miniaturized so the impedance of the solution is higher than the resistance of the nanoparticle film. In a study by Wieczorek and coworkers [27], the detection of analytes in water was demonstrated (Figure 1.5). On an interdigitated electrode where there was a separation between electrodes, 6-nm gold nanoparticles were deposited. Once deposited, the nanoparticles were modified with 1-hexanethiol by exposing the surface to 1-hexanethiol vapors. The nanoparticle-modified surfaces were then exposed to an aqueous solution containing varying amounts of chloroform. The impedance signal was shown to vary with the concentration of chloroform. As for the switching time, this was demonstrated by exposing the nanoparticle modified film to an aqueous solution containing toluene and showed a 10-s switching from the detection to the absence of toluene in the film. Reproducibility was also demonstrated by exposing the nanoparticle film to a series of aqueous solutions containing toluene, which showed repeatable signals upon each consecutive exposure. Wieczorek and coworkers [27] demonstrated that the device had a fast response time, good repeatability and sensitivity down to 0.1 ppm.

Changing the resistance between two electrodes using nanoparticles has also been applied to the detection of large biomolecules. In a study by Velev and Kaler [28] latex nanoparticles modified with protein A, a receptor for the immunoglobulin molecule, were aggregated onto the gap between two electrodes (Figure 1.6). The surface was then exposed to immunoglobulin G (IgG). After the binding of the IgG molecules to

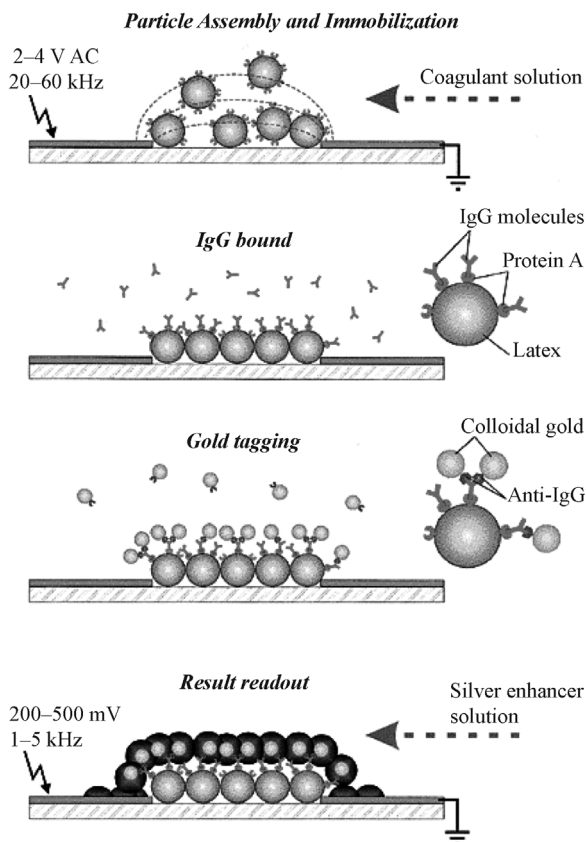


**Figure 1.6** Schematic of the main stages of sensor assembly and functioning, demonstrated by an immunoglobulin test. (Reprinted with permission from Ref. [28]. ©1999 American Chemical Society.)

the nanoparticles, the surface was exposed to anti-IgG-modified gold nanoparticles. The gold nanoparticles acted as seeds for the deposition of silver, which linked the two electrodes with a concomitant increase in conductivity between the two electrodes. When a current was passed through this layer the resistance ranged from 50–70  $\Omega$  in the wet state and 40–50  $\Omega$  in the dry state. The electrodes that had negative controls, meaning no formation of the antibody–antigen bond, had resistances of  $10^3 \Omega$ . The experiment was also repeated with biotin–streptavidin biological molecules, which showed similar results to the above. Velev and Kaler concluded that the method developed in this study is as sensitive to those of clinical assays. Also, the detection limit of a few tens or hundreds of molecules is possible due to the low number of gold nanoparticles required to create the link between the two electrodes.

The use of nanoparticles to form bridges between two electrodes was also utilized to detect DNA hybridization, including single base-pair mismatches, by Mirkin and

coworkers [29]. In this case DNA-modified gold nanoparticles were used to seed the silver deposition. The setup for the device is to firstly modify the glass substrate in the gap between the two gold electrodes with succinimidyl 4-(maleimidophenyl)-butyrate, then the capture DNA was immobilized onto the activated glass surface. The target DNA formed a bridge between the surface-bound capture DNA and the DNA on the gold nanoparticles. Thus, in the presence of target DNA a network of gold nanoparticles will form between the two electrodes. Finally, a deposition of silver completed the setup, linking the two gold electrodes and resulted in a reduction in the resistance. The study demonstrated the ability to detect a single base pair mismatched by a less significant reduction of resistance compared with a fully complementary DNA strand. Another feature that this concept demonstrated was the exquisitely low detection limit for DNA (500 fM of DNA). With the reduction of the gap between the electrodes and a narrower conducting channel between the two electrodes it is possible that even higher sensitivities, as demonstrated by Lieber *et al.* with nanowires, may be possible [30, 31].

Narrower conducting channels can be fabricated by dip-pen nano lithography (DPN) [32]. Basnar *et al.* [33] have shown the possibility of the use of DPN to deposit gold nanoparticles modified with glucose oxidase enzymes and the subsequent growth of these gold nanoparticle by the enzymatic reaction with glucose (Figure 1.7). In this study, the enzyme glucose oxidase was modified with *N*-hydroxysuccinimide functionalized gold nanoparticles. This solution of glucose oxidase gold nanoparticle aggregate was used as an ink to deposit the aggregate at a specific location using DPN. Once deposited, a solution of glucose and  $\text{AuCl}_4^-$  was exposed to the enzyme layer. The reaction of glucose to gluconolactone resulted in the reduction of  $\text{O}_2$  to  $\text{H}_2\text{O}_2$ . The  $\text{H}_2\text{O}_2$  then reacted with the  $\text{AuCl}_4^-$  to deposit gold onto the glucose oxidase conjugated gold seed nanoparticles (a concept previously demonstrated by Willner and coworkers [34]). The process resulted in the growth of the gold nanoparticles such that they merged and formed a conducting wire. Willner and coworkers [33] have also concluded that with the application of other biocatalytic inks it is possible to extend the concept into production of semiconducting polymers, magnetic nanowires, semiconductor nanowires and insulating polymers.

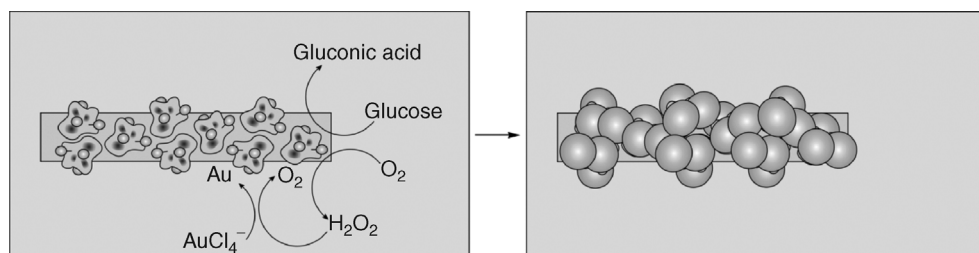


**Figure 1.7** General scheme for the formation of Au nanowires created by DPN, using flavoenzymes. (Reprinted with permission from Ref. [33] ©2006 Wiley-VCH Verlag GmbH & Co. KGaA.)

## 1.2.2

**Templating using Membranes**

Although nanoparticles can increase the surface area of an electrode, the positioning of these nanostructures is difficult to control. An alternative way that allows for greater control of positioning of nanostructures is templating. Templating not only provides greater control over the locality of nanostructures but provides opportunities for a different range of shapes to be produced, such as tubes [35–37], rods [35, 36, 38, 39] and wells [21, 38–41]. The first example of producing nanostructures using templates was by Martin and coworkers [35], where polypyrrole was templated in a track-etched polycarbonate membrane or porous alumina membrane. Both types of membranes are commercially available, but each has different advantages with regards to producing nanostructures. Track-etched templates are produced by an initial bombardment of the membrane material with nuclear fission particles followed by further chemically etching. These membranes have uniform pores of sizes down to 10 nm in diameter and with pore densities as high as  $10^9$  pores per square centimeter. However, one drawback of these membranes is the pores are randomly distributed. Alumina membranes, on the other hand, have pore sizes that are uniform and distributed in a hexagonal pattern (Figure 1.8). These templates are produced electrochemically using aluminum metal and have pore densities up to  $10^{10}$  pores per square centimeter [42]. This high pore density has the advantage that it allows for higher surface area nanostructures to be templated. The pore sizes that are commercially available, however, are limited to a minimum of 20 nm diameter. As a consequence, Martin and coworkers [43] have developed electrochemical strategies for the production of a range of pore sizes with the smallest being 5 nm.

The deposition of a conductive polymer (polypyrrole) into either a track-etched polycarbonate or alumina membrane was either achieved by electrochemical reduc-

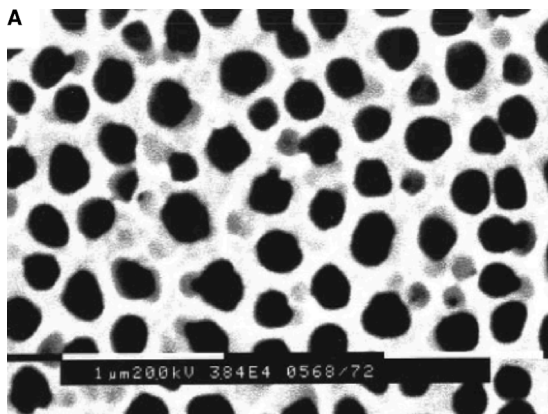


**Figure 1.8** SEM image of porous alumina membrane, used in templating. (Reproduced by permission of The Royal Society of Chemistry from [36].)

tion [44] or chemical deposition [45, 46]. For example, the electrochemical synthesis of polypyrrole [44] can be achieved by the reduction of the pyrrole monomers in the presence of the membrane and a metal anode. Martin and coworkers [44] used an alumina template upon which they sputter coated one side with a thick layer of Au that covered the entrance to the pores. Following this process, the Au membrane film was placed in epoxy with only the area to be templated exposed. This template was then placed into a pyrrole solution to electrodeposit polypyrrole. Depending on the length of the desired tubes the time of current application is varied. The diameter of the tube is determined by the size of the membrane structure. Once the reduction of polymer is complete the membrane is then dissolved to expose the nanotubes. The produced nanofibrillar electrode demonstrated slightly higher current density (3–7%) when compared to unstructured electrodes. The magnitude of the increase in current density is greater as the nanofibers become narrower. The largest increase in current density recorded was one order of magnitude [45].

An alternate method to produce templated electrodes is the use of chemical reduction of the monomer in the presence of a track-etched or alumina membrane. Parthasarathy *et al.* [46] have produced enzyme-loaded nanotubules by a combination of both electrochemical and chemical deposition. Initially, the alumina membrane was sealed at one end with a thick Au film (Figure 1.9a), after which the membrane was placed into a mixture of pyrrole and  $\text{Et}_4\text{NBF}_4$ . The pyrrole was then electropolymerized to form a small plug of polypyrrole at the closed end of the alumina membrane (Figure 1.9b). Subsequently, the membrane was placed into a

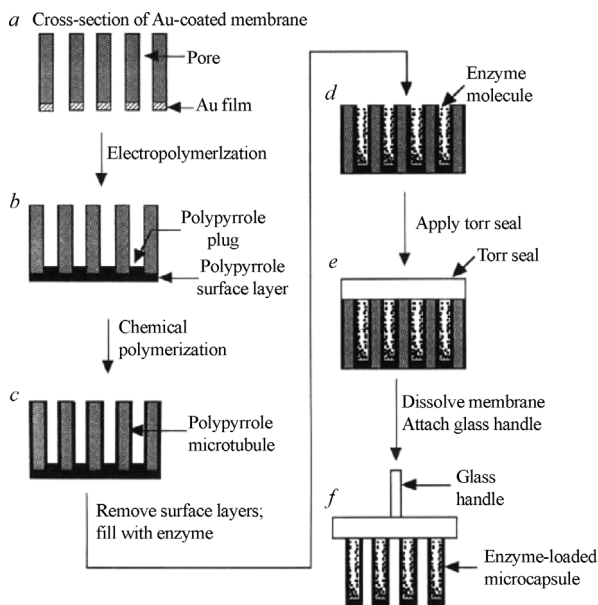


**Figure 1.9** Schematic diagram for the method used to produce and enzyme load microcapsule arrays. (Reprinted with permission from Ref. [46]. ©1994 Nature Publishing Group.)

mixture of pyrrole and chemically polymerized. The resultant structure conformed to the shape of the membrane (Figure 1.9c). The enzyme was then loaded (Figure 1.9d) and finally the open end was sealed off with a Torr seal (Figure 1.9e). Once the Torr seal is dried, the membrane was removed to reveal an array of polypyrrole plugged tubes that contained the immobilized enzyme in their interior (Figure 1.9f). Placement of this electrode into a solution of  $\text{H}_2\text{O}_2$  showed decomposition of the  $\text{H}_2\text{O}_2$  to  $\text{O}_2$  and  $\text{H}_2\text{O}$ , suggesting the polymer is porous to the biological analyte,  $\text{H}_2\text{O}_2$ .

In a related study by Contractor and coworkers [47] similar structures were produced but without the chemical polymerization step. The production of the structure used a polycarbonate membrane, where first a thin layer of Au was deposited over the top and bottom surfaces of the membrane (Figure 1.10a). Upon

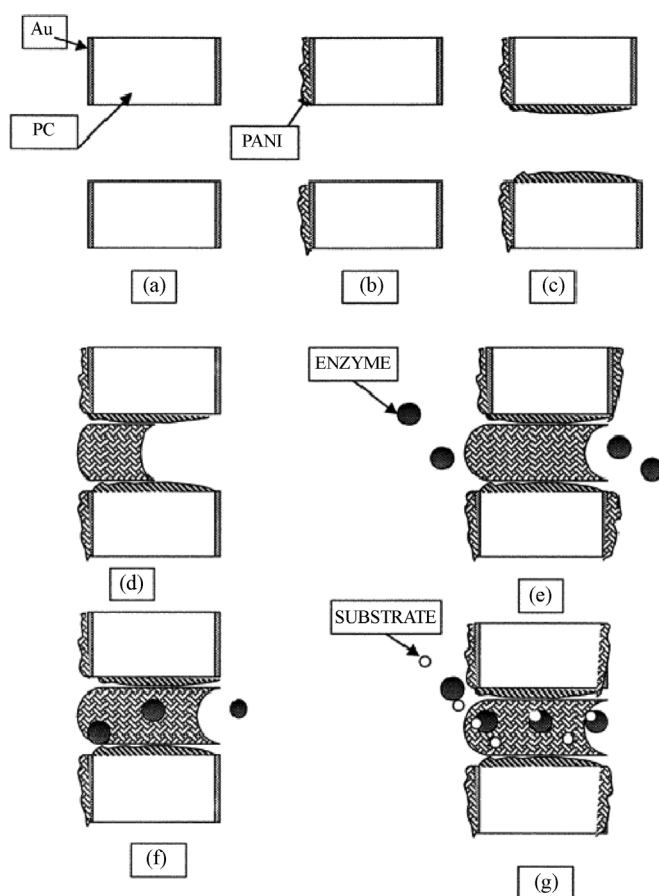


**Figure 1.10** Production scheme for polyaniline nanotubes, loading of enzymes into the tubes and finally exposure to an analyte. (Reprinted with permission from Ref. [47]. ©1999 American Chemical Society.)

transferring the membrane to a 0.1 M aniline solution the Au-coated membrane was cycled between  $-0.2$  and  $+0.8$  V vs. SCE to produce polyaniline tubes (Figures 1.10b–d). Once this was completed the tubes were exposed to the enzyme and immobilized in a solution containing 0.1 M aniline (Figures 1.10e–g). The completed nanostructured electrode could be connected on the front and back (source and drain), creating a potential drop across the polymer film. This potential drop allowed for the controlled oxidation of the polyaniline, as a result amplifying the reduction of the polyaniline by the enzymatic reaction when reacting with  $\text{H}_2\text{O}_2$ . The produced nanostructured electrode showed excellent performance capabilities, sensitivity and response rate. These capabilities are a combination of three factors (1) small source and drain separation improving the transduction ability, (2) disorder in the polyaniline microstructure, resulting in large changes in conductivity on switching of the polyaniline and (3) a large loading of the enzyme, resulting in faster diffusion of substrate to the enzyme.

The differently produced conductive polymer structures described above all have enhanced conductivity, which can be employed in microelectronics [44] and as sensors using immobilized enzymes [46, 47]. Martin and coworkers used polarized infrared absorption spectroscopy to access the alignment of the polymer fibers on the outer surface of the nanotubes [48]. The study showed that the enhancement of the conductivity is due to the alignment of the polymer fibers on the outer surface of the tubes.

Production of nanostructured electrodes by templating is restricted not only to conducting polymers but also to a range of other materials including metals [35, 38, 41, 49], metal oxides [39], and semiconductors [40]. Although conductive polymers are easily templated, the electrical and optical properties exhibited by the nanostructuring are limited. This is in contrast to nanostructured metals, which have demonstrated unique optical and electronic properties [35, 50, 51]. This was demonstrated by Martin and coworkers using an alumina template to nanostructure gold tubules, by three techniques, electrochemical deposition [35], chemical reduction from solutions [51] and direct sputtering into the alumina membrane [41, 52].

The electrochemical technique entails the use of an alumina template, which has been surface modified with (2-cyanoethyl)triethoxysilane [50]. Before the electrodeposition of Au onto the surface, a 50-nm layer of Au was sputtered onto one end of the membrane (Figure 1.11a:A). This sputtering did not close the pores but converted the alumina template into an electrode. Following the sputter treatment the membrane was placed into a commercially available gold-electroplating solution (Orotemp 24, Technics) and a current density of  $0.5\text{--}2.0$  mA cm $^{-2}$  was passed through the membrane (Figure 1.11a:B and C). After the growth of the tubes was completed the alumina membrane was dissolved to reveal the gold tubules (Figure 1.11a:D). Due to the modified membrane surface the growth of the gold that was being deposited does not favor the formation of fibers but tubes. Martin and coworkers have reported tube lengths as long as  $2\text{ }\mu\text{m}$  can be produced by this method. The gold nanostructure within the alumina films showed very interesting optical properties. Due to the alumina membrane being transparent the color of the film produced is a direct result of the gold nanofibers produced within the

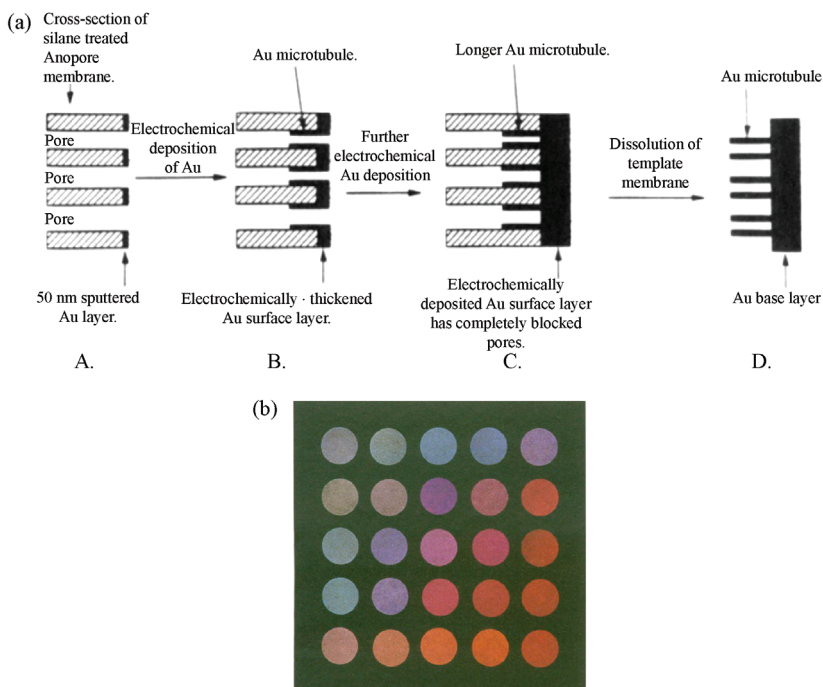


**Figure 1.11** (a) Stepwise production of metallic nanotubes, where the internal surface area was modified with (2-cyanoethyl)triethoxysilane, followed by electrochemical deposition and removal of the alumina template. (Reprinted with permission from Ref. [50]. ©1991 American Chemical Society.) (b) Optical properties of gold nanotubes in alumina membranes at various sizes and lengths. (From [35] C.R. Martin, *Science*, 266, (1994), 1961–1966. Reprinted with permission from AAAS.)

membrane. Similar to free-standing gold nanoparticles where the color is size dependent (smaller-sized nanoparticles give a blue shift, larger size a red shift) the same can be said for the nanotubes within alumina membranes. Martin and coworkers have synthesized a range (20–150 nm diameter and various lengths) of gold nanotubes within alumina membranes (Figure 1.11b). This study demonstrated the color dependence on size, where the wider nanotubes showed a blue shift, but as the nanotubes became longer there is a red shift in the observed color.

In a related study, silver microtubules were produced by chemical deposition [38]. Similar to electrochemical deposition, the surface of the membrane must first be modified, not with a silane but with a catalyst such as  $\text{Sn}^{2+}$  ions. Initially, one side of the membrane is protected by tape (Figure 1.12b) and then the surface is activated with  $\text{SnCl}_2$  (Figure 1.12c). The activated membrane was then placed into a solution of silver-plating solution (Figure 1.12d). This resulted in the deposition of silver over the activated surface; finally the alumina membrane was dissolved away.

Direct sputtering of the desired metal into an alumina membrane to give arrays of nanotubes has also been achieved. This was demonstrated by Guo *et al.* [41] where by controlling the sputter rate and pressure of the chamber it was possible to

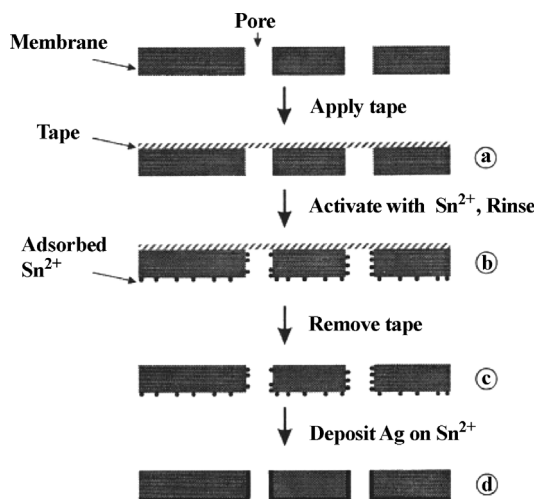


**Figure 1.12** Stepwise synthesis scheme for chemical deposition of silver into an alumina membrane. (With kind permission from Springer Science + Business Media: [38]. A. Huczko, Applied Physic A, 70, (2000), 365–376 Figure 1.7 Reprinted with permission from The Materials Research Society.)

directly deposit metals into the porous structure of an alumina membrane. In this study the alumina membrane was placed at an angle, which was normal to the sputtering beam. Initially, the membrane was coated with a layer of gold, which was  $\sim 100$  nm in thickness at a sputtering rate of  $0.05$  nm/s and a pressure of  $8.7 \times 10^{-5}$  Pa. Following this slow deposition the rate was increased to  $0.2$  nm/s at a pressure of  $4.4 \times 10^{-4}$  Pa (Figure 1.13a). This deposition closed the pores and deposited a further  $200$  nm of gold on top of the film (Figure 1.13b). The membrane was then dissolved away with sodium hydroxide leaving behind an array of nanotubules on a surface of Au (Figures 1.13c and d). This array of nanotubules exhibited an electroactive surface area of  $2.4$  times that of the geometric area. With an increase in the electroactive area, it becomes possible to apply these arrays to the area of sensors, electrochemical analysis and catalysis.

Other structures have been produced apart from metallic nanotubules. Nanorods have also been produced employing electrochemical deposition. Hong and coworkers [52] have used alumina membranes to produce gold nanorods, which have been shown to have high catalytic responses to biologically important analytes. In this study the nanostructured surface was produced by first etching a glass surface with argon plasma followed by an initial  $50$ -nm sputtered layer of platinum and a further  $100$ -nm layer of gold. The gold surface was then modified with the alkanethiol cysteamine. An alumina membrane was placed onto this cysteamine-modified surface and gold was then electrodeposited. Upon the removal of the alumina membrane in sodium hydroxide, a nanostructured electrode of gold nanotubes was produced. The nanostructured electrode was demonstrated to have a  $4.6$  times higher electroactive surface area than that of the unmodified, flat gold electrode. Apart from

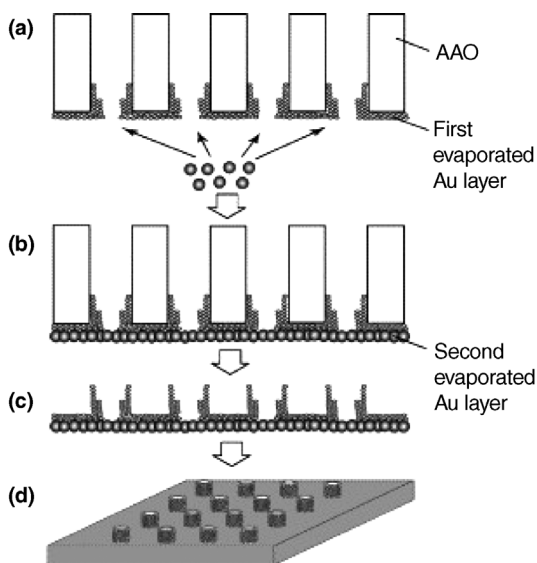


**Figure 1.13** Stepwise synthesis of direct gold sputtering onto alumina membrane to produce nanostructures. (Reprinted with permission from Ref. [41]. ©2005 Elsevier.)

the increased surface area, the nanostructured electrode also exhibited catalytic characteristics, allowing for the electrode to be used as an enzyme-free sensor for glucose (oxidation begins at 0.1 V vs. Ag|AgCl for bare electrodes and  $-0.25$  V vs. Ag|AgCl for nanostructured electrodes),  $\text{H}_2\text{O}_2$  (reduction commences at  $-0.26$  V vs. Ag|AgCl on nanostructured electrodes and  $-0.61$  V vs. Ag|AgCl for flat electrodes) or  $\text{O}_2$  ( $-0.06$  V vs. Ag|AgCl on a nanostructured electrode). The porous structure, in combination with the catalytic response demonstrated by the electrodes, allows for the discrimination of glucose from other interfering agents, ascorbic acid, uric acid and acetamidophenol.

Membrane templates have been used extensively to create other high surface area structures. In recent years the application of polycarbonates and alumina membranes has been used to template electrodes for batteries [39] and capacitor devices [40]. For example, Sides and Martin have used membranes to produce  $\text{V}_2\text{O}_5$  nanofibers for enhanced performance of Li-ion batteries in low temperatures. The production of the nanostructured film entails the use of a polycarbonate membrane. This polycarbonate membrane was placed over the top of a metal electrode, and then a solution of the  $\text{V}_2\text{O}_5$  precursor tri-isopropoxyvanadium (TIVO) filled the pores. The TIVO was hydrolyzed to  $\text{V}_2\text{O}_5$ , excess  $\text{V}_2\text{O}_5$  was removed simply by wiping with a cotton swab and finally the nanostructured electrode was placed in an  $\text{O}_2$  plasma for 2 h to remove the polycarbonate template. The nanostructured  $\text{V}_2\text{O}_5$  electrode surface showed much better low-temperature performance, which was most evident at  $-20^\circ\text{C}$ . Martin and coworkers [39] suggest that the enhanced performance at low temperatures is due to a decrease in diffusion coefficient within the electrode nanostructure.

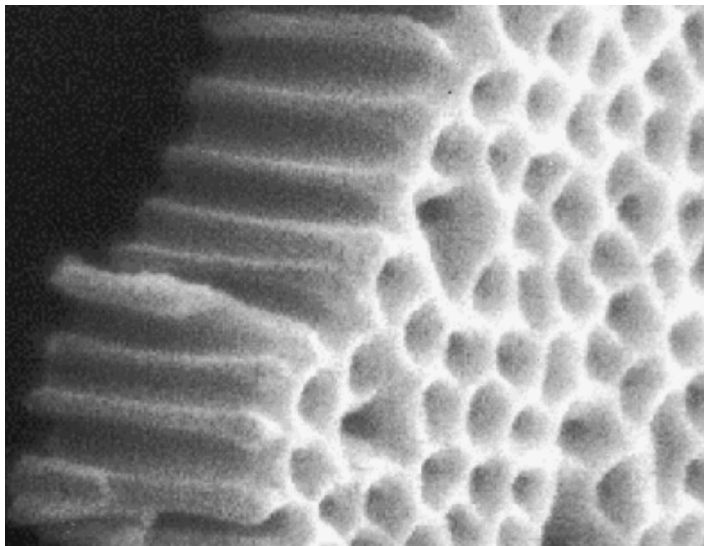


**Figure 1.14** SEM image of honeycomb-structured alumina onto a carbon electrode before O<sub>2</sub> plasma exposure. (Reprinted with permission from Ref. [40]. ©2003 The Electrochemical Society.)

Martin and coworkers [40] have also employed alumina membranes in the production of high surface area carbon electrodes in the shape of honeycomb structures for capacitors. In this study the electrode was produced by the use of alumina membranes. First, the pores of the membrane were widened with an Ar plasma. After this etching, the alumina membrane was placed over the top of a carbon electrode (Figure 1.14). This assembly was then placed into a plasma mixture of O<sub>2</sub> and Ar and was exposed for 2 min. During this time the O<sub>2</sub> plasma propagated through the alumina membrane to the carbon film located at the bottom. This plasma etching produced a structure on the carbon electrode that mimicked the alumina membrane used. This electrode was tested in terms of discharge rate and capacity. Martin and coworkers [40] observed a low-rate discharge capacity of 325 mAh g<sup>-1</sup>. However, at high rates, delivery of 50 times the capacity of an unmodified electrode was observed. This high rate of discharge is due to the increased surface area and is required for the application of high discharge devices, as is the case in electric car acceleration.

### 1.2.3

#### Templating using Lyotropic Liquid Crystals

Membrane templating is capable of producing a range of structures in various sizes. However, the degree of control is not at the molecular scale. An alternative templating method that has molecular-level control over the pore size and the ability to produce ordered arrays of pores is lyotropic liquid crystal templates [53]. Lyotropic liquid crystals are surfactant phases produced at high percentages of surfactant to solvent.

If the solvent is polar, the surfactant forms self-assembled structures with the headgroups remaining in contact with the polar solvent and the hydrophobic tails maintain their contact with each other and away from the solvent. Depending on the ratio of surfactant to solvent different periodic surfactant nanostructures are possible. For example, structures produced with a normal topology hexagonal ( $H_1$ ) phase contain cylindrical self-assembled surfactant rods arranged in a close-packed hexagonal fashion. However, if the cubic phase (Ia3d) was used, interconnected cylindrical rods that form a gyroid lattice are produced [53]. Attard and coworkers [54] have demonstrated the ability to produce nanostructured metals such as Pt films using lyotropic liquid crystals as a templating technique. In this initial study lyotropic liquid crystals were used to template the production of nanostructured platinum films. The surfactant octaethyleneglycol mono-hexadecyl ether was first used to form a hexagonal mesophase, which was stable at room temperature. In the continuous water phase hexachloroplatinic acid was dissolved. A large piece ( $>3$  mm) of a less-noble metal (Fe, Zn Mg) was placed into the liquid crystal, which reduced the platinum precursor. The mixture turned black when the reaction was left to stand at room temperature for 24 h. These particles were imaged using a TEM (Figure 1.15), which revealed that the particles have a close-packed hexagonal nanostructure consisting of pores, which have a diameter of 3 nm in size and a surface area of up to  $23 \text{ m}^2 \text{ g}^{-1}$ , which is much greater in comparison with flat platinum films where the surface areas is  $4.5 \text{ m}^2 \text{ g}^{-1}$ .

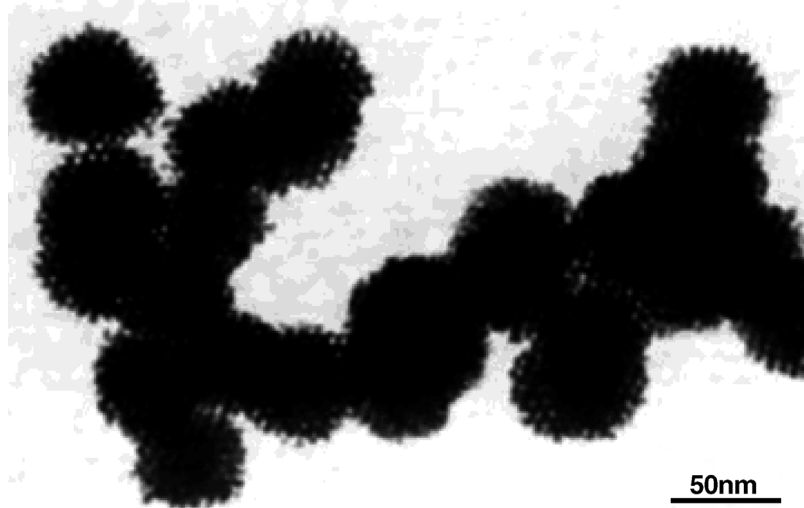


**Figure 1.15** TEM image of Pt nanoparticles that have been produced by lyotropic liquid crystal templating. Porous structures can be seen and are spaced in an hexagonal array. (Reprinted with permission from Ref. [54]. ©1997 Wiley-VCH Verlag GmbH & Co. KGaA.)

Utilizing the ability of lyotropic liquid crystal as templates to produce high surface area and arrayed structures, Attard and coworkers [53] applied the concept to the production of nanostructured electrodes by electrodeposition. In this study the use of a nonionic surfactant octaethyleneglycol monohexadecyl ether was employed with hexachloroplatinic acid to produce a H<sub>1</sub>-templated platinum structure on the surface of a flat gold electrode. The resulting electrodeposited structure had pore sizes of ~2.5 nm, but using the same strategy and placing nonpolar solvents caused a swelling of the surfactant rods, thus increasing the pore size to 3.5 nm. This platinum film had a higher surface area of 20 m<sup>2</sup> g<sup>-1</sup> compared to flat platinum films, which have a surface area of 4.5 m<sup>2</sup> g<sup>-1</sup>. As for electrochemical properties, due to the higher surface area a much higher capacitance of 5.2 × 10<sup>-2</sup> F cm<sup>-2</sup> was also observed in comparison to flat platinum electrodes, which have a capacitance of 1.2 × 10<sup>-2</sup> F cm<sup>-2</sup>. Attard *et al.* [53] concluded that the production of metallic films by lyotropic liquid crystals showed enhanced electrochemical properties. Also, the ability to tune the size and spacing of the pores was demonstrated.

There has been a range of materials that have been templated by lyotropic liquid crystals other than platinum including polymers [55], Pd [56], Zn [57], Cd [57], Ni [58], Sn [59] and Co [60]. Apart from the range of materials that can be templated with lyotropic liquid crystal, the electrodes have also been proposed to find applications in fuel cells [53], batteries, hydrogen storage [56] and sensors [61]. These applications typically exploit the high surface area and or electrocatalytic properties of these electrodes. An example is templated palladium electrodes for hydrogen storage. Denuault and coworkers [56] demonstrated the use of a nanostructured palladium electrode for use in hydrogen adsorption. The synthesis of the electrode was once again achieved using electrodeposition of (NH<sub>4</sub>)<sub>2</sub>PdCl<sub>4</sub> from a H<sub>1</sub> phase liquid crystal where the surfactant was either octaethyleneglycol monohexadecyl ether or Brij 56 (46 weight %). The highly pure octaethyleneglycol monohexadecyl ether gave more ordered structures compared with the Brij 56 where the surfactant possessed a broader range of molecular weights. However, the majority of the structures produced in this study were made by using Brij 56 due to the cost being ~88 times less than the ether and yet the same average properties were achieved. Once the lyotropic liquid crystal structure was in equilibrium, the palladium was electrodeposited onto a flat platinum electrode. This nanostructured electrode demonstrated a much larger electroactive surface area of 300 times, when compared to the unmodified electrodes. This study showed the adsorption of hydrogen gas was rapid due to the catalytic properties and large surface area. The electrode also showed an excellent potentiometric response over a pH range of 2–12.

The high surface areas of these electrodes make them ideal for electroanalytical applications where the high surface area is exploited to improve detection limits and/or detection range. Evans *et al.* [61] have demonstrated the production of platinum mesoporous electrodes and their application into the detection of H<sub>2</sub>O<sub>2</sub>. The produced electrode had an internal surface area that was ~100 times higher than the original electrode. The study demonstrated a larger detection range of 0.02–100 mM H<sub>2</sub>O<sub>2</sub> compared to the unstructured electrode, which had a range of 0.02–40 mM. This broader range can be ascribed to the larger surface area

giving a larger number of surface sites for the hydrogen peroxide to adsorb and undergo oxidation. Apart from the enhanced surface area Evans *et al.* [61] also observed an improvement in the surface catalytic property.

#### 1.2.4

#### Colloidal Templates

Nanoparticles have also been used as template nanostructured surfaces. The main advantage that nanoparticle templating has over membranes or lyotropic liquid crystals is simply the huge range of materials and sizes that can act as templates. The challenge, however, is to form ordered arrays of colloids on surfaces. This approach will not be discussed in detail here but to demonstrate the benefits of the strategy one example will be illustrated. In a study by Sun *et al.* [62] the production of a porous  $\text{SnO}_2$  film by templating with a polystyrene (PS) nanoparticle monolayer was demonstrated. The production of the porous film from a nanoparticle template entailed firstly the spin coating of the polystyrene nanoparticles onto a flat glass substrate. Following the spin coating the monolayer film of PS nanoparticles were floated off the glass slide onto the top of a  $\text{SnCl}_4$  solution. The film was then lifted off the surface of the  $\text{SnCl}_4$  solution by a glass rod and heat treated. This deposition process was repeated 4 times to form the final electrode to detect ethanol vapors. Characterization under TEM of the surface revealed a network of pores arranged in a close-packed hexagonal array (Figure 1.16).

In normal air, the  $\text{SnO}_2$  can adsorb oxygen species of  $\text{O}_2^-$ ,  $\text{O}^-$  and  $\text{O}^{2-}$  on the surface, which increased the resistance of the  $\text{SnO}_2$  nanostructured film [63]. Sensing of ethanol vapors was completed in a  $300^\circ\text{C}$  environment. At this temperature the ethanol vapor reacts with the oxygen species on the surface of the  $\text{SnO}_2$  and removes

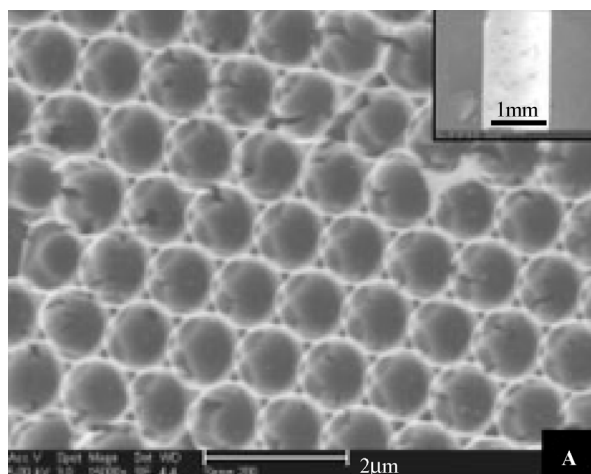


**Figure 1.16** TEM images of  $\text{SnO}_2$  ordered porous films on the external surface of a glass tube. (Reprinted with permission from Ref. [62]. © 2005 Wiley-VCH Verlag GmbH & Co. KGaA.)

the oxygen from the surface, and as a result decreases the resistance in the film. The production of porous films with smaller (200 nm) PS nanoparticles showed a 7-fold increase in sensitivity and additionally led to a response rate that was 5 times faster response when compared to a similar film produced by larger particles (1000 nm). This significant increase in sensing is attributed to the increased surface area.

### 1.3

#### Catalytic Properties

Recent rapid developments in nanoparticle preparation, surface modification and assembly have led to the widespread use of nanostructures immobilized on electrodes to catalyze electrochemical reactions [64]. While a diverse range of reactions have been shown to be electrocatalytically enhanced by nanostructured electrodes, this section will focus on reactions that involve the direct electron transfer between electrodes and redox-active molecules of biological relevance. Such enhancement of electron transfer has facilitated the development of biosensors for direct quantification of the redox-active biomolecule, with greater sensitivity, wider detection limits and decreased response times. The effective quantification of biological molecules using nanostructured electrodes requires that nanostructures attached to electrodes are able to electrochemically catalyze redox reactions of the biological molecules. Electrodes functionalized for this purpose can be broadly categorized into metallic-nanoparticle and carbon-nanotube structures. This section will highlight the key advances in the synthesis and performance of metallic-nanoparticle nanostructured electrodes for biological reactions.

The use of metallic nanostructures to enhance direct electrocatalysis of a biological molecule has developed in parallel to carbon nanotubes. Gold nanoparticles were the first example of this application owing to their ease of fabrication and well-known electrocatalytic and conductive properties. This was demonstrated by Jin and coworkers [65] who immobilized ~14-nm gold nanoparticles on cysteine-modified platinum electrodes coated with a thin film of Nafion. The electrode displayed excellent catalytic activity towards nitric oxide (NO), a physiological messenger and cytotoxic agent. Differential pulse voltammetry (DPV) showed large increases in current response for gold nanoparticle-modified electrodes along with cathodic shifts of oxidation peaks in comparison to bare platinum electrodes due to the catalytic oxidation of NO. The enhanced electrocatalytic ability of the nanostructured electrode was attributed to the gold nanoparticles acting as 'electron antennae', which efficiently funnel electrons between the electrode and electrolyte. The Au nanostructured electrodes also showed linear current response with increasing NO concentrations, selectivity to NO and detection limits of  $5.0 \times 10^{-8}$  mol/L NO, making the use of such electrodes for NO quantification very attractive.

A different example of gold-nanoparticle-modified electrodes for NO detection was shown by Caruso and coworkers [66]. In this work, the layer-by-layer technique was utilized as a means to immobilize oppositely charged layers of gold-nanoparticle-loaded poly(sodium 4-styrene-sulfonate) (PSS) and poly(allylamine hydrochloride)

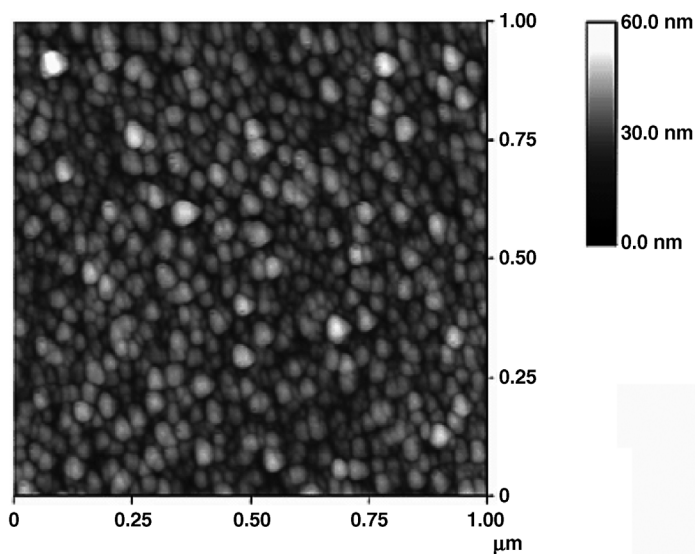


**Figure 1.17** AFM image of a gold-nanoparticle-loaded polyelectrolytes film. (Reprinted with permission from Ref. [66]. ©2003 American Chemical Society.)

(PAH) (Figure 1.17) onto indium tin oxide (ITO) electrodes. This approach allowed for fine control of the amount of Au nanoparticles bound on the electrode surface. The system was again applied to the detection of NO using sodium nitrite ( $\text{NaNO}_2$ ) as the precursor of NO and it was shown that the sensitivity of the electrode could be improved by increasing the gold nanoparticle content through the deposition of more polyelectrolyte layers.

The use of organic molecules or polymers to assist in binding nanoparticles to electrodes was highlighted as possibly having adverse effects on electrode catalytic reactivity and conductivity [67]. The influence of the organic binding molecules on the conductivity of nanoparticle-modified electrodes is clearly demonstrated for nanoparticle resistance sensors discussed in Section 1.2.1 above. With this in mind, Oyama and coworkers [68] attempted to reduce the interference of organic binders on electrode performance by using a two-step approach. This approach involved the initial immobilization of gold seed nanoparticles onto an ITO electrode followed by reductive growth of the seeded particles. Electrochemical impedance spectroscopy used in this study demonstrated convincingly that there was a significant enhancement of charge transfer for a gold nanoparticle/ITO electrode compared to a gold nanoparticle/ITO electrode with a 3-mercaptopropyltrimethoxysilane (MPTMS) linker. To show the biological applicability of this new approach, Oyama and coworkers [69] tested the electrocatalytic performance of a gold nanoparticle/ITO electrode for the direct electrochemical detection of a wide range of biological molecules including, paracetamol, uric acid, ascorbic acid, guanosine and the catecholamines epinephrine, norepinephrine and dopamine. In all the cases, comparison of cyclic voltammograms between gold nanoparticle/ITO electrodes

and bare electrodes show a cathodic shift in the oxidation peaks for these biomolecules as well as an enhancement of peak current, both of which provide evidence of the electrocatalytic properties of gold nanostructures on electrodes. Selectivity of the electrode in the presence of interfering molecules, however, was sometimes found to be an issue for these gold nanoparticle/ITO electrodes [69].

Further development of the use of gold nanostructures to enhance biological electrocatalysis involved the use of different polymer binders on the surface to enhance selectivity of the electrodes. One such study by Lin and coworkers [70] used overoxidized polypyrrole (PPyox) to immobilize gold nanoclusters onto a glassy-carbon electrode (GCE), for the simultaneous quantification of epinephrine and uric acid in the presence of ascorbic acid. The PPyox in this case acted as a molecular sieve and allowed for the resolution of three distinct peaks for each of the analytes, which was not previously possible. In another study, poly(3,4-ethylenedioxythiophene)-poly(styrene sulfonic acid), (PEDOT-PSS) was spin coated onto an ITO electrode followed by the electrochemical deposition of gold nanoparticles into the polymer matrix for NADH oxidation [71]. The use of PEDOT-PSS is attractive because it easily forms thin films through many conventional techniques. In this study, Lee and coworkers show that the gold nanoparticle/PEDOT-PSS-modified ITO electrodes displayed high selectivity and sensitivity for NADH, making these nanostructured electrodes particularly attractive for NADH-sensing applications as well as in those that use NADH as a cofactor for enzymatic reaction.

A novel extension of utilizing gold nanostructures for electrocatalysis was the demonstration by Yu and coworkers [72] of electrocatalytic gold nanowires (Figure 1.18). The carbon-nanotube-inspired gold nanowires were synthesized through templated electrodeposition. The gold nanowires were then dispersed in a chitosan matrix and deposited onto a GCE (Figure 1.18). The gold nanowire electrode was found to provide excellent electrochemical response and also was found

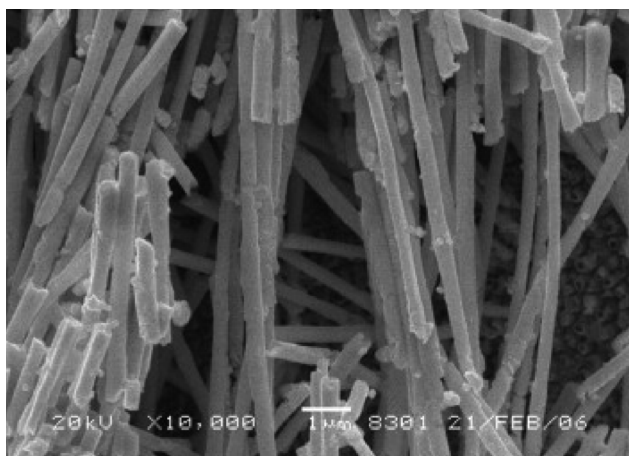


**Figure 1.18** SEM image of the electrodeposited gold nanowires in a chitosan matrix. (Reprinted with permission from Ref. [72]. ©2007 Elsevier.)

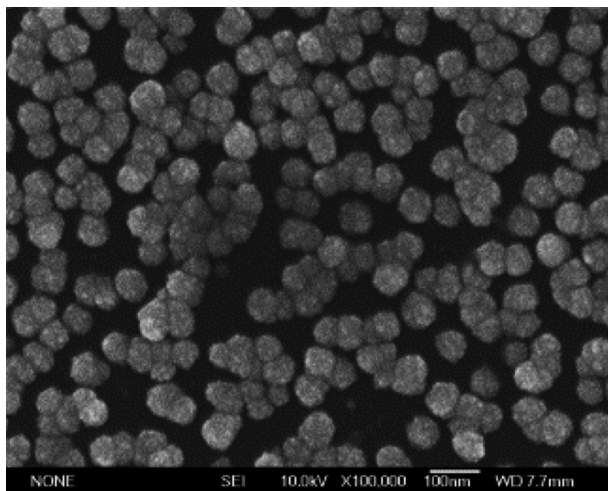


**Figure 1.19** SEM image of the Pt/Fe(III) cooperative composites immobilized on a Nafion-coated GCE. (Reprinted with permission from Ref. [74]. ©2004 Elsevier.)

to be 30 times more sensitive to  $\text{H}_2\text{O}_2$  than a conventional gold electrode. These enhancements were attributed to the higher effective surface area resulting from the immobilization of the gold nanowire structures on the electrode as well as their unique electrical properties and high conductivity.

Other metallic materials that have been used to produce nanostructured electrodes for biological electrocatalysis include platinum, platinum/iron composites and copper [73–75]. The nanostructured electrodes in these studies were produced either by electrodeposition of nanoparticles onto Nafion-modified electrode surfaces, [73, 74] or by covalent binding using MPTMS as a linker molecule [75]. Lin and coworkers showed that the use of platinum/Fe(III) nanoparticles on a Nafion-coated GCE could be used for the selective detection of NO (Figure 1.19), while Selvaraju and Ramaraj immobilized platinum nanoparticles on a Nafion-coated GCE for the detection of dopamine and serotonin. As in the case of gold nanostructured electrodes, the platinum nanostructures enhanced the catalytic and conductive properties of the electrodes by acting as ‘electron antennae’, while the Nafion coating acts as an ion-selective membrane, giving rise to the enhanced selectivity. It should be noted, however, that the polymeric coatings result in a reduced electrocatalytic response when compared to nanostructured electrodes without these coatings. This makes the decision to use such coatings a tradeoff between electrocatalytic ability and selectivity of the electrode. The electrocatalytic performance of copper nanoparticles immobilized on ITO electrodes was also studied for NO detection by Wang and coworkers [75]. They found that copper nanoparticles showed an enhanced electrocatalytic response to NO and displayed a wider linear detection range when compared to the gold nanoparticle/polyelectrolyte films synthesized by Caruso and coworkers [66]. The selectivity of the nanostructured electrode was not explored, however, and this remains an issue for electrodes that do not have chemoselective polymer coatings.

## 1.4

### Exploiting Nanoscale Control to Interface Electrodes with Biomolecules

As discussed above nanomaterials can provide electrocatalytic properties. However, one unique property that can be achieved by nanostructuring electrodes with conducting elements that are of the order of just a few nanometers or less is the opportunity to perform electrochemistry in confined spaces. Such a possibility is particularly attractive for interfacing electrodes with biomolecules. Interfacing electrodes with biomolecules is important for biosensing, biofuel cells and other bioelectronic devices [13, 76–78]. In the case of both biosensing with redox enzymes and the employment of redox enzymes in biofuel cells one of the main challenges is electronic communication with the biomolecules. It is this process that is the limiting factor in the performance of both types of devices. This is perhaps most ably demonstrated with the glucose biosensor where the enzyme glucose oxidase is interfaced with an electrode. To allow transduction in such enzyme electrodes, electrons are shuttled between the enzyme and the electrode by freely diffusing redox molecules. The need for this freely diffusing molecule is not only the rate-limiting step but is also the source of many of the problems these devices face with regards to reproducibility and interferences [79]. As a consequence, there is a considerable research effort motivated towards achieving direct electron transfer to proteins [80–83]. The main challenge in achieving direct electron transfer to proteins is that in most proteins the redox-active center is located deep within the redox protein [84]. For example, in the case of glucose oxidase the redox-active center, flavin adenine dinucleotide, is located about 20 Å from the surface of the glycoprotein [85]. Such distances are too far for appreciable electron transfer to occur. Two possible strategies for ‘wiring’ redox proteins to overcome this distance problem are to either (1) nanostructure electrodes with nanomaterials that are sufficiently small that they can penetrate the proteins and reduce the distance electrons must tunnel to the electrode or (2) nanostructure electrodes with organic molecules that can plug into the proteins and serve as conduits for electron transfer [86]. We will discuss these two strategies in turn.

#### 1.4.1

##### Plugging Nanomaterials into Proteins – Nanoparticles

The modification of electrodes with nanoparticles followed by the attachment of redox enzymes is one approach to nanostructuring electrodes that has been successful at achieving direct electron transfer to enzymes. Perhaps the most stunning example of this approach is to use nanoparticles to wire into glucose oxidase, as has been achieved by Willner and coworkers [87]. In this work, a gold electrode was modified with a dithiol self-assembled monolayer such that one thiol attached to the gold electrode and the other to gold nanoparticles, which were 1.4 nm in diameter. Active glucose-oxidase-modified gold nanoparticles were produced in one of two ways (Figure 1.20). In the first the redox-active center of glucose oxidase, flavin adenine dinucleotide (FAD), was immobilized onto a SAM-modified

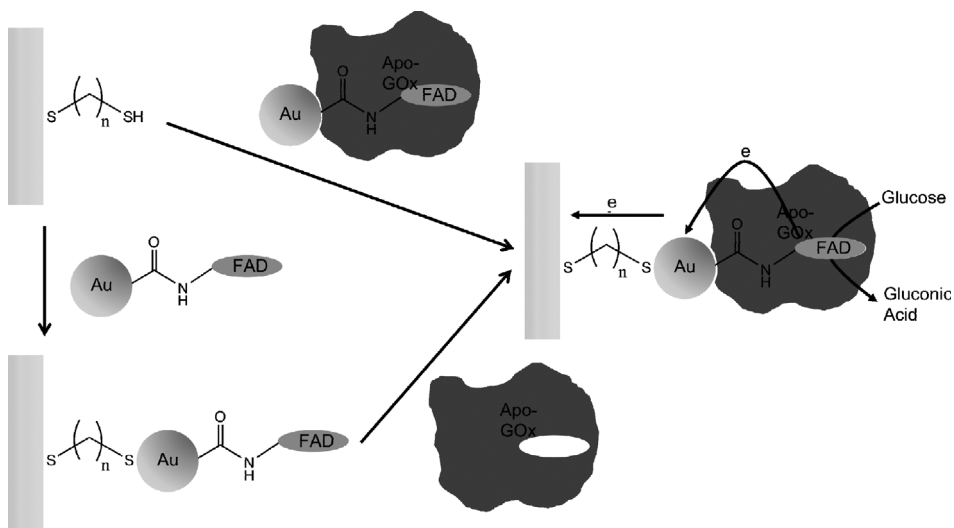


**Figure 1.20** Assembly of Au-nanoparticle-reconstituted GOx electrode by adsorption of Au-nanoparticle-reconstituted GOx onto a dithiol monolayer and a stepwise build-up of the electrode by deposition of the Au-nanoparticle FAD onto the dithiol surface followed by the reconstruction of the apo-GOx.

nanoparticle that was subsequently attached to the electrode. The active enzyme was produced by reconstitution of the apo-enzyme around the FAD-modified nanoparticle attached to the electrode surface. In the second approach, the enzyme was reconstituted onto the FAD-modified nanoparticles in solution prior to attaching the nanoparticle to the electrode surface. Both strategies produced active enzyme and enzyme electrodes where direct electron transfer to glucose oxidase could be achieved with almost identical performance. The electrode performance itself was outstanding. The enzyme electrode responded to glucose in the absence of oxygen at a rate seven times the maximum rate observed in nature when oxygen recycles the enzyme. Furthermore, the rapid rate was also regarded as an explanation for the fact that there was no apparent influence of either oxygen (the natural cosubstrate for the enzyme) or ascorbic acid in the sample on the performance of the enzyme electrode. The mechanism by which direct electron transfer to the enzyme's redox-active center is not yet explained, although it is logical to assume the size of the nanoparticles are important. Within this paper the impact of nanoparticle size was not explored although it was stated in the paper that the nanoparticles must be of appropriate dimensions. The particles used in this paper were only 1.4 nm in diameter, which is significantly smaller than the dimensions of glucose oxidase of  $5.5 \times 6 \times 8$  nm [85]. Thus, it seems possible that the nanoparticles allow the refolding of the enzyme into its native configuration and the covalent link between the nanoparticle and the active center allows appreciable electron transfer to occur [88].

What the Willner study highlights is the enormous possibilities of connecting electronic elements to proteins using nanoparticles. In particular, the absence of

interferences from oxygen and ascorbic acid with this enzyme electrode provides strong support for the notion that efficient direct electron transfer to enzymes such as glucose oxidase could solve many of the problems associated with diffusing redox species shuttling electrons between the enzyme and the electrode. Other workers have also demonstrated fast electron transfer to enzymes using nanoparticle assemblies but typically these electrodes have employed enzymes with redox-active centers close to the exterior of the protein. As far back as 1996, Natan and colleagues [89] modified tin oxide electrodes with gold colloids and showed direct electron transfer to cytochrome *c*. The tin oxide electrodes were modified with a self-assembled monolayer of (3-aminopropyl) trimethoxysilane, whereupon the colloids were exposed to the electrode and adsorbed via bonding between the amine and the particles. The electrochemistry of cytochrome *c* was explored at these electrodes with the most significant result being the demonstration of a size dependence of the electrochemistry; a phenomenon alluded to in the Willner work [87]. In a similar example, Liu *et al.* [90] have modified graphite electrodes with silver nanoparticles to enable rapid electron transfer to cytochrome *c*. In this example the pyrolytic graphite electrode was oxidized in permanganate. Cysteamine was then attached to the carboxylic acid functionalized surface via its amine. Silver nanoparticles of 11 nm in diameter were then attached to the thiol end of the electrode and cytochrome *c* adsorbed onto this surface. The ability of nanoparticles to facilitate electron transfer over very long distances was shown by Ulstrup and coworkers [91] when they used 3 to 4-nm diameter gold-nanoparticle-modified gold electrodes to electrochemically interface with cytochrome *c*. They showed that enhanced rates of electron transfer were achieved but more significantly that electron transfer could proceed at an appreciable rate over distances of greater than 50 Å.

#### 1.4.2

#### Plugging Nanomaterials into Proteins – Carbon Nanotubes

Carbon nanotubes have also been used to facilitate wiring of enzymes, again exploiting the small size of these nanomaterials as electrodes that can penetrate close to the active site of the enzymes. The first example of this strategy was by Guiseppi-Elie and coworkers [92] where carbon nanotubes were randomly dispersed onto a glassy-carbon electrode, whereupon glucose oxidase was adsorbed onto the electrode. With this very simple electrode construct direct electron transfer to the enzyme was achieved with a rate of electron transfer of  $1.7 \text{ s}^{-1}$ , which is significantly faster than that reported when immobilizing glucose oxidase onto a self-assembled monolayer modified gold electrode where a rate of  $0.026 \text{ s}^{-1}$  has been reported [93]. The fast rate constant for electron transfer was attributed to the small size of the single-walled carbon nanotubes employed (typically only 1 nm in diameter [94]). It is noteworthy that an almost identical rate constant was reported by Zhao *et al.* [95] using nanotube-modified electrodes prepared in a very similar way.

Work on the nanostructuring of electrodes with carbon nanotubes by Gooding and coworkers [96, 97] has demonstrated that superior electrochemical performance can be achieved with carbon nanotubes that are vertically aligned compared with being

randomly dispersed. Aligning carbon nanotubes can be achieved in one of two ways. The first method is by growing the nanotubes vertically off a surface [98–103]. This strategy, however, usually produces multiwalled carbon nanotubes that are possibly too large to penetrate enzymes, however, it is possible as single-walled carbon nanotubes (SWNTs) have been grown off a surface [104]. The other method is via self-assembly using strategies developed by Liu and coworkers [105–107] and extended by others [96, 108–112]. In this strategy, SWNTs are purified in concentrated acids that open the closed ends such that they are terminated with carboxylic acid moieties [106]. The surface chemistry of the electrode surface is then tailored to allow the carboxylic acid moieties to bind to give aligned nanotubes. These aligned carbon nanotube arrays were first interfaced with enzymes by Gooding *et al.* [108]. In this case an array of perpendicularly oriented SWCNTs on a gold electrode was fabricated by covalently attaching carboxylic acid functionalized SWCNTs, generated by the oxidative scission of the carbon nanotubes, to a cysteamine monolayer-functionalized gold electrode. The enzyme microperoxidase MP-11 was attached to the distal ends of the SWCNTs. The efficiency of the nanotubes acting as molecular wires was determined by calculating the rate constant of heterogeneous electron transfer between the electrode and microperoxidase MP-11 attached to the ends of the SWCNTs. A variety of different length distributions were assembled onto the electrode to explore the distance dependence of electron transfer through these nanotube arrays. What the paper showed was that the length distribution of nanotubes assembled on the electrodes had very little impact on the apparent rate of electron transfer compared with transferring the electrons from the redox-active center to the nanotube; thus highlighting the efficiency of electron transfer through the nanotubes and hence that nanotubes can serve as nanoscale electrodes as described in Chapter 3. At the same time, using a similar strategy of CNTs aligned by self-assembly, Yu *et al.* [109] reported that quasireversible  $\text{Fe}^{3+}/\text{Fe}^{2+}$  voltammetry was observed for the iron heme enzymes, myoglobin and horseradish peroxidase.

An exciting extension of this idea of assembling enzymes onto the ends of carbon nanotube electrodes was to plug the electrodes inside proteins. This has been achieved by both Willner and coworkers [110] and by Liu *et al.* [113] with surprisingly similar results considering the complexity of the systems. In both cases plugging the nanotubes inside glucose oxidase was achieved by first covalently attaching the FAD cofactor carboxylic groups at the free ends of the aligned SWCNTs. Apo-glucose oxidase was then reconstituted around the FAD units linked to the ends of the standing SWCNTs, in a similar manner to that for interfacing nanoparticles with glucose oxidase, to give the active enzyme [110, 113]. Willner and coworkers measured the interfacial electron-transfer rate constants to be  $83 \text{ s}^{-1}$ ,  $42 \text{ s}^{-1}$ ,  $19 \text{ s}^{-1}$ , and  $12 \text{ s}^{-1}$ , for assemblies that include standing SWCNTs of mean length 25 nm, 50 nm, 100 nm, and 150 nm average length, respectively. Thus, the nanotube length did influence the electron-transfer rate between the FAD units and the electrode in this case.

The rate constants for electron transfer achieved by plugging the nanotubes into the proteins as described above are an order of magnitude or more greater than those reported by Guiseppi-Elie *et al.* [92] and Zhao *et al.* [95] when interfacing wild-type

glucose oxidase with the randomly dispersed carbon nanotubes. Similarly, they are significantly faster than that reported by Liu *et al.* [113] where wild-type glucose oxidase was adsorbed onto aligned carbon-nanotube-modified electrodes. These studies therefore highlight the importance of plugging the nanotubes into the enzyme and forming a direct covalent link with the redox-active center of the protein. They also highlight the importance of the size of the nanoscale features on an electrode such that they can connect to the redox center of the protein without disrupting the ability of the protein to refold into an active form.

### 1.4.3

#### Plugging Nanomaterials into Proteins – Molecular Wires

The importance of forming a direct link between the redox center and the underlying electrode has been shown numerous times with organic monolayers by Willner and coworkers [114–117] where redox relays form a connection between a macroscopic electrode and FAD whereupon apo-glucose oxidase is assembled over the surface-bound redox-active center. The nanotube approach, however, makes the connection by using the nanotube essentially as a molecular wire. Gray and coworkers [118–120] have demonstrated excellent connectivity to the redox-active centers of enzymes using conjugated organic molecular wires. In the first example of this approach electrodes were modified with a self-assembled monolayer of rigid oligo(phenyl-ethynyl)-thiol molecular wires that contained diethylaniline at the distal end (Figure 1.21) [120]. Oligo (phenyl ethynyl) and related conjugated molecular wires have been shown to allow very rapid electron transport due to the extended conjugation of  $\pi$ -electron and the rigidity of the molecules [9, 121, 122]. The enzyme amino acid oxidase, another enzyme with flavin adenine dinucleotide (FAD) as the redox-active center, was adsorbed onto this interface and the electrochemistry of FAD in its natural position buried deep within the wild-type enzyme was investigated. Remarkably, a lower limit of the rate constant of electron transfer was  $1000 \text{ s}^{-1}$ , which is consistent with other electron-transfer studies through these types of molecules [121, 122] but unprecedented for electron transfer to redox enzymes. This incredibly rapid rate confirms that there is excellent electronic coupling between the FAD and the electrode despite the molecular wire being 22 Å long. This excellent electronic coupling is because the molecular wire is designed to bind directly to the redox-active center of the enzyme. The diethylaniline at the distal end of the molecular wire was chosen as it is a known inhibitor of amine oxidase. Thus, the binding of the diethylaniline terminus in the active site serves to direct the molecular wire close to the active site; hence enabling efficient electron transfer through the molecular wire between the electrode and FAD.

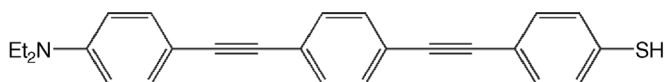


**Figure 1.21** Molecular wire: rigid oligo(phenyl-ethynyl)-thiol molecular wires that contained diethylaniline at the distal end.

The interfacial design used in the study of Hess *et al.* [118] is not only important for interfacing electrodes with redox proteins but because it demonstrates three important recent advances for nanostructuring electrodes that offer unique properties. These three concepts are (1) using binding moieties on a monolayer surface to ensure intimate connectivity with biomolecules, (2) using rigid molecules that extends the capability of nanofabrication on surfaces by allowing coupling to the interior of nanoscale features and (3) the use of molecular wires in electrochemistry such that long-distance electron transfer can be exploited for a variety of applications. We will discuss each of these three features in turn.

#### 1.4.3.1 Nanostructuring Electrodes to Achieve Intimate Connectivity with Biomolecules

Waldeck and coworkers [123, 124] had previously explored this concept using alkanethiol SAMs terminated with different moieties at the omega position and determined the best connectivity to cytochrome *c* was achieved with pyridine-terminated SAMs [125]. Armstrong and coworkers have also recently employed a similar strategy for interfacing graphite electrodes with blue copper oxidase (laccase) enzymes, where graphite electrodes are modified with an anthracene diazonium salt where the diazo group was on the 2 position. The reductive adsorption of aryl diazonium salts has been shown to produce very stable layers on carbon electrodes [126–128] and here will give anthracene-modified electrodes (Figure 1.22). The anthracene molecules were shown to bind the laccase enzymes tightly via the hydrophobic,  $\pi$ -electron-rich, binding pocket. The resultant laccase-modified electrode showed excellent performance, with the current density for the electrocatalytic reduction of oxygen at least twice as large as for laccase adsorbed onto unmodified graphite electrodes. Electroactivity was retained with repeated cycling, indicating the laccase was strongly attached to the electrode and the electrode demonstrated long-term stability (catalytic activity being 57% of the original current density after 8 weeks). An important aspect of this electrode modification was the orientation of the anthracene on the electrode. If the diazo moiety was on the 1 position, such that the anthracene was less able to protrude from the electrode surface, no catalytic enhancement was observed.

#### 1.4.3.2 Nanostructuring Electrodes using Rigid Molecules

The correct orientation and rigidity of the anthracene is also related to the second important idea in the nanostructuring of the electrode interface used by

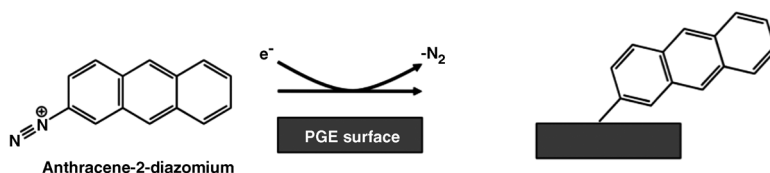


**Figure 1.22** Anthracene-2-diazonium deposition by an electrochemical means. (Reproduced by permission of The Royal Society of Chemistry from [129].)

Hess *et al.* [118]; that is the use of rigid molecules to allow surface assembly onto electrodes that would not be possible with flexible molecules. When using SAMs for nanofabrication of a surface in a stepwise manner (that is sequentially adding additional components to the surface one after another rather than forming the entire molecular system and then assembling it) the common strategy is to use either a single component or a mixed SAM of multiple components. Mixed SAMs are used to allow lateral spacing of the coupling points such that their surface density can be controlled, which can be particularly important if the material to be assembled onto the surface has a larger footprint than the individual SAM forming molecules. The distance of the assembled species from the underlying electrode surface is defined by the thickness of the SAM. Because of the flexibility of the individual molecules in the SAM, close packing of molecules is required to define the distance. Hence, if one of the components is longer than the other species in the SAM then the distance from the surface is defined by the major component (Figure 1.23). That is, if the shorter component is the minor component then it will be buried within the SAM [130]. Alternatively, if the longer component is the minor component, its flexibility means that the distance from the surface is still defined by the shorter component and connectivity of the SAM to a nanoscale feature is still limited to the exterior of the material being coupled. Rigid molecules on the other hand can protrude from the interface as if they are molecular posts (Figure 1.23). Using such molecules the opportunity exists for connections to be made to the interior of nanomaterials (Figure 1.23).

In connecting the diethylaniline into the redox-active center of the amine oxidase in the study by Hess *et al.* [118] the connection is made possible for the connection to be made to the interior of the enzymes because the molecules were rigid. However, for this to occur requires sufficient spacing between the molecular wires on the

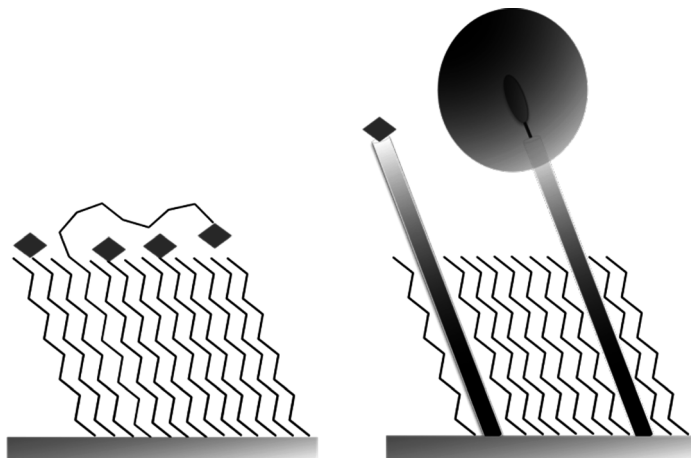


**Figure 1.23** Scheme of long aliphatic molecules to project redox molecules above the environment (left) and the utilization of rigid molecules to probe into proteins and project redox molecules above the SAM surface (right).

electrode surface to ensure that the enzymes fit over the molecular wires. In the interfacial design by Hess *et al.* [118] the molecular wires have not been separated by a diluent but only 75% of the surface was reported to be covered by the molecular wires. The coverage of the enzyme was determined voltammetrically to be only 25% of a monolayer. This low coverage may in fact reflect the locations on the surface where there is sufficient space for the enzyme molecules to slide over the rigid molecular wires or alternatively the surface may be covered by a monolayer of enzyme but connectivity is not made to all enzymes.

The Gooding group has extended this concept of using rigid ‘molecular posts’ in the formation of hybrid enzyme–electrode constructs using both oligo (phenyl ethynyl) molecular wires [131, 132] and norbornylogous (NB) bridges [133, 134] as minor components in a mixed self-assembled monolayer where the major component was significantly shorter than the molecular post. In this way, the molecular posts stand proud above the plane of the SAM with sufficient space between the posts such that individual posts can connect to sites in the interior of large biomolecules. This strategy is illustrated in Figure 1.24 for achieving direct electron transfer to glucose oxidase [132] using a mixed layer of an oligo (phenyl ethynyl) molecular wire and a benzoic acid diluent, where both molecules on the surface were derived from aryl diazonium salts. The enzyme is allowed to adsorb onto the interface, whereupon it is anchored to the electrode using standard carbodiimide coupling. If this coupling procedure is performed then stable peaks in the cyclic voltammograms attributed to flavin adenine dinucleotide within the protein are observed with a half-wave potential of  $-443\text{ mV}$  versus  $\text{Ag|AgCl}$ . Without the

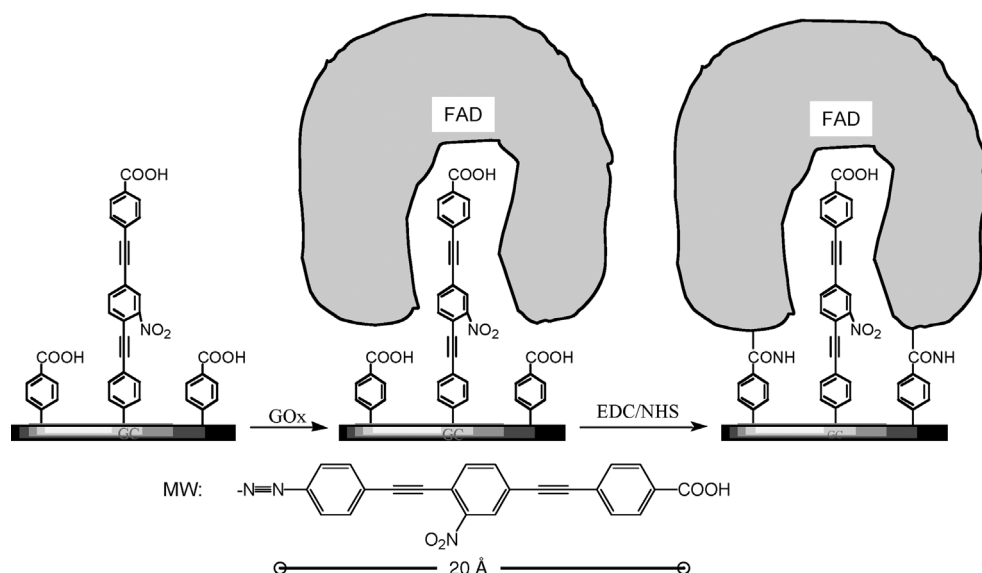


**Figure 1.24** Scheme for the use of rigid molecular wires to plug into enzymes. (Reprinted with permission from Ref. [132]. ©2007 Elsevier.)

anchoring step the electrochemistry was observed to be unstable. The rate constant for electron transfer was calculated to be  $78 \text{ s}^{-1}$ , which is a massive enhancement in rate compared with the  $1.6 \text{ s}^{-1}$  reported in other studies on direct electron transfer to wild-type glucose oxidase using graphite electrodes [135] and carbon-nanotube-modified electrodes [92, 95]. This high rate is because the molecular wire is thought to penetrate close to the active site via the channel through which the glucose gets to the active site. The entrance of the active site is approximately  $10 \text{ \AA}$  in diameter [85], which is sufficient to allow the molecular wire to at least partially penetrate the protein towards the active site without denaturing the enzyme. The important aspects of this study were firstly the enzyme was shown to be able to turn over glucose in the absence of oxygen or any other freely diffusing mediating species, which indicates the enzyme is being turned over by direct electron transfer, and secondly that enzyme turnover was occurring at  $-400 \text{ mV}$  versus  $\text{Ag}|\text{AgCl}$ . This turnover potential is the most negative yet recorded for direct electron transfer to glucose oxidase, which has important consequences for fuel cells where the more cathodic the potential of the anode the greater the power output.

With regards to interfacial design, the molecular wires on the surface are diluted using a short carboxy phenyl derivative, which as mentioned above also serves to anchor the protein to the surface. Changing the ratio of the two components in solution was shown to be able to influence the amount of glucose oxidase interrogated electrochemically at the electrode surface. The optimal ratio in the assembly solution was 1 : 30 molecular wire:carboxy phenyl derivative. At this ratio there was a surface coverage of glucose oxidase, as determined from the voltammetric peaks, of  $2.4 \text{ pmol cm}^{-2}$ . This surface coverage is consistent with the coverage of GOx ( $2.6 \text{ pmol cm}^{-2}$ ) on 3-mm diameter GC electrodes determined by radioactive  $^{125}\text{I}$  labeling [136] and this value is only just below the theoretical maximum coverage of a monolayer of GOx of between  $2.6$  and  $3.8 \text{ pmol cm}^{-2}$  [137] that was calculated from the crystallographic size of GOx of  $5.5 \times 7.0 \times 8.0 \text{ nm}$  [85]. Increasing the ratio of molecular wires results in a decrease in surface coverage that is attributed to the surface density of molecular wires crowding the interface such that there is insufficient spacing between wires to allow all the enzymes attached to the surface to fit over a wire and at lower ratios of molecular wires there are insufficient number of wires to get a complete monolayer of enzyme immobilized.

As a final aside in this section, it is important to note that carbon-nanotube-modified electrodes where the carbon nanotubes are vertically aligned, the nanotubes can essentially be exploited in the same basic way as molecular posts. That is, in essence, what was demonstrated in the examples by the Willner group and the Gooding group into plugging carbon nanotubes into glucose oxidase. In these cases the small size and the rigidity of the carbon nanotubes were crucial for the success of these enzyme-wiring strategies.

#### 1.4.3.3 The use of Molecular Wires in Electrochemistry such that Long-Distance Electron Transfer can be Exploited for a Variety of Applications

The final aspect of the electrode design in the work by Hess *et al.* [118] is the use of molecular wires for modified electrodes for applications other than molecular

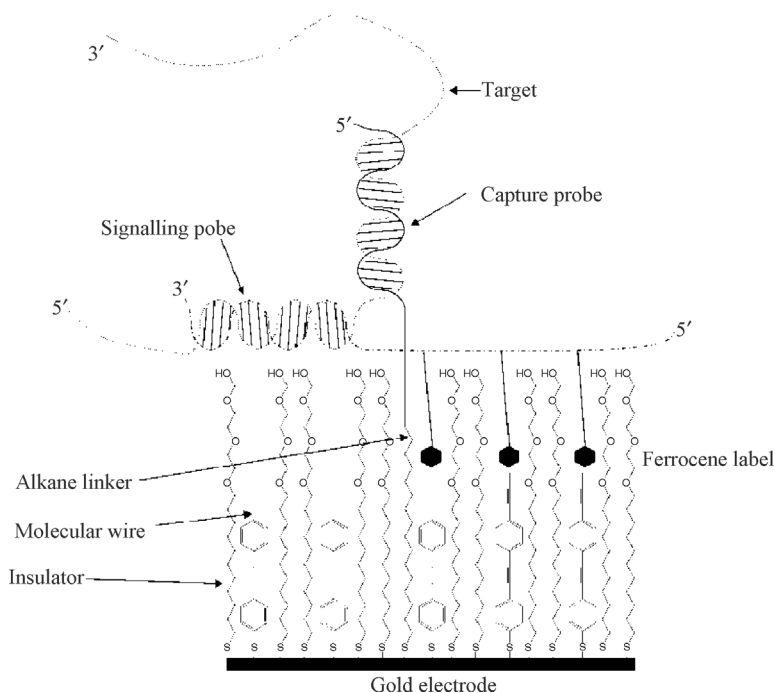


**Figure 1.25** Scheme for the use of molecular wires to sense DNA hybridization where a capture DNA is used to attract the target DNA and then a signal DNA with ferrocene labels is hybridized to signal the hybridization event. (Reprinted from [138]. *Mol. Diagn.* 2001 3: 74–84 with permission from the American Society for Investigative Pathology and the Association for Molecular Pathology.)

electronics. This was not the first use of molecular wires in such a way that the concept has been previously demonstrated in the Clinical Microsensors (CMS) DNA biosensor [138] (Figure 1.25). The self-assembled monolayer used to modify the electrode to give it selectivity for DNA comprised three components. These were (1) thiolated DNA molecules to selectively detect complementary strands of DNA in the sample, (2) an oligoethylene glycol (OEG)-terminated alkanethiol as an antifouling layer that resists nonspecific binding of DNA and proteins and (3) oligo (phenylethynyl) thiols as the molecular wires to allow electrochemical communications to the underlying electrode.

Liu and Gooding have adapted this type of interface for protein electrochemistry and to allow electrochemistry to be performed in biological media without electrode fouling [131]. As with the interface for probing direct electron transfer to glucose oxidase by the same workers the self-assembled monolayers were derived from aryl diazonium salts reductively desorbed onto a glassy-carbon electrode rather than alkanethiols on gold. The reason for using aryl diazonium salts [128, 139] is that they form much more stable layers on carbon and metal surfaces than the alkanethiol

system [128, 140]. As with the CMS system the molecular wire allows electrochemical communication with the electrode and the OEG molecules resist nonspecific adsorption of proteins to the surface. The ability of the interface to ensure proteins are selectively attached to the molecular wires was shown using horseradish peroxidase (HRP), a protein to which direct electron transfer can easily be achieved. The electrochemistry of the heme center shows a close to ideal full width half-maximum ( $E_{\text{FWHM}}$ ) for the oxidation peak. The close to ideal  $E_{\text{FWHM}}$  is good evidence that all the proteins being interrogated electrochemically are in the same environment, which essentially means the only enzymes that are wired to the electrode are those covalently attached to the molecular wires.

The crucial aspect of this interface is that the oligoethylene-glycol-terminated molecules passivate the electrode such that species in solution cannot access the underlying electrode. Hence, the oligophenylethynyl molecules are absolutely necessary for any electrochemical response. What the antifouling layer and molecular wire in combination does, however, is to bring the design of electrode interfaces into the realms of interfaces in optical detection [141] where interactions of proteins with the surface can be precisely controlled. This has not been previously possible because in most electrode constructs the electrode interface must be open and accessible to freely diffusing species such that electrochemical signals can be achieved. The drawback of allowing electroactive species to diffuse to the electrode surface is that if any other species in solution are electroactive at the same potential then they will become interferences. As this interface does not require access of diffusing species to the electrode surface the interface also serves the function of preventing these electroactive interferences reaching the electrode and solving this long-standing problem.

The monolayer construct in Figure 1.24 has already been shown to have advantages for DNA biosensors [138], protein electrochemistry [131] and immunosensing [142] but its potential has yet to be touched for performing electrochemistry in complex biological media such as found in cell-culture media. The important features of this system for performing electrochemistry in complex media are the highly stable aryl diazonium salt SAMs, the protein resistance and restriction of electroactive interferences from accessing the electrode surface. The challenge is to configure the interface with a biorecognition molecule that can be attached to the molecular wire that will allow detection of an analyte of interest. This is the challenge we are now pursuing.

Liu *et al.* [140] have also used this interface for an electrochemical immunosensor for small molecules (Figure 1.26). In this sensor, one end of the molecular wire is attached to ferrocene dimethylamine with a covalent link formed between one of the amine groups on the ferrocene and the carboxyl group on the wire. To the other amine is attached the antibody-binding epitope for the antibody, in this proof-of-concept study the epitope is biotin. Electron transfer can be readily achieved to the ferrocene molecule but upon antibody binding to this interface, the electrochemical signal is dramatically reduced.

The immunosensor based on the modulation of electrochemical signals by protein binding can be used in two modes. The first is to detect the presence of antibodies in a



without requiring the user to perform any tasks other than expose the sample to the sensor. The sensing concept is general for any small molecule so could be applied to analytes such as drugs or pollutants.

The interfacial design and the presence of the antifouling layer are absolutely vital for the success of this sensing concept. Evidence has been provided that the attenuation of the electrochemistry is due to restricting the access of ions to the ferrocene to balance the charge once the ferrocene is immersed in protein [134, 142]. As a consequence, any nonspecific adsorption of protein to the interface will also cause an attenuation in electrochemistry. Hence, the antifouling layer is required to ensure the attenuation of the electrochemistry associated with the presence of antibodies is due to a specific interaction with the binding epitope on the molecular wire rather than any nonspecific effects. The ability of this layer to resist nonspecific adsorption of proteins, as well as preventing electroactive species reaching the electrode, was demonstrated by Liu and Gooding [131] previously and is demonstrated in the current paper via controls that show there is little attenuation in the ferrocene electrochemistry if a different antibody is used or if the biotin epitope is absent from the interface.

## 1.5 Switchable Surfaces

### 1.5.1 Switching Properties of Monolayer Systems

SAMs containing two or more constituent molecules provide a practical experimental system with which to generate model systems to study fundamental aspects of the interactions of surfaces with biological systems. The primary advantage that SAMs (especially mixed SAMs) have over other methods of creating organic surfaces (polymer films, adsorbed proteins) is that the chemical composition of the surface can be modified in a deliberate manner. The other key advantage is the spatial control that SAMs afford. One of the most dramatic examples of this spatial control is a reversibly switching surface developed by Langer and coworkers [143, 144]. The basic idea is shown in Figure 1.27. A gold surface was modified with an alkanethiol SAM with a labile head group that had a footprint larger than the size of the alkyl chain such that the molecules could not close pack on the electrode surface. Removal of the labile headgroup left a hydrophilic mercaptohexadecanoic-acid-modified surface. The spacing between the molecules on the surface was such that each molecule occupied an area of about  $0.67 \text{ nm}^2$ , which was greater in comparison to a close-packed surface where each molecule occupies an area of  $0.29 \text{ nm}^2$ . The greater spacing between molecules was necessary to allow room for the mercaptohexadecanoic acid to bend towards the underlying gold surface. Application of an electrical potential was used to control the orientation of SAM molecules on a gold electrode surface, which can reversibly switch the surface between two conformations and hence two properties. A potential positive of the point of zero charge attracted the negatively charged

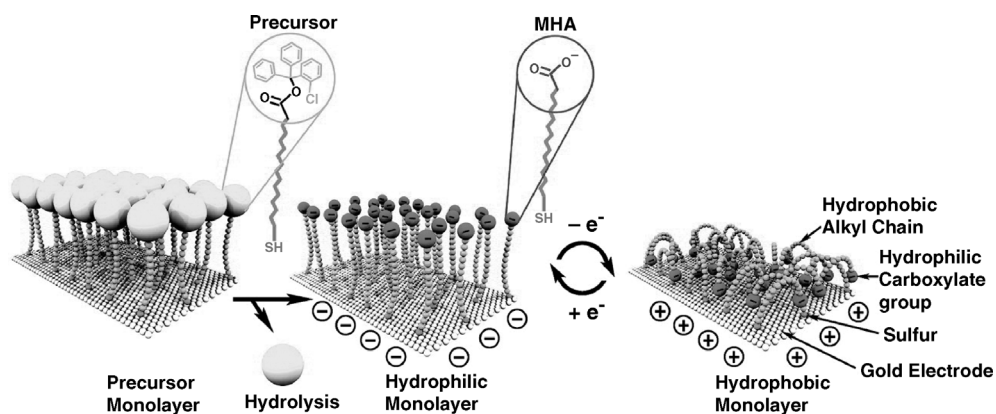


**Figure 1.27** Scheme showing the use of charged head groups to 'switch' between hydrophilic and hydrophobic surfaces by changing the potential applied to the surface. (From [144] J. Lahann, S. Mitrogotri, T.N. Tran, H. Kaido, J. Sundaram, I.S. Choi, S. Hoffer, G.A. Somorjai and R. Langer, *Science*, 299, (2003), 371–374. Reprinted with permission from AAAS.)

carboxylic acid moieties at the distal end of the SAM to the electrode surface. The bending of the molecules towards the electrode resulted in the surface changing from presenting carboxylic acids to alkyl chains to the exterior, which caused a change in character of the electrode from hydrophilic to hydrophobic. This change in orientation altered the wettability of the surface almost instantaneously. A similar approach was explored by Willner and coworkers [145, 146] where the distal group on the SAM was a dipyrindinium species. The essential difference was that the attraction and repulsion was not purely electrostatic as the distal moiety was also redox active. Hence, upon switching to a positive potential the distal species was also oxidized and when switching negatively the redox-active group was reduced. Thus, although still reversible switching, the Willner study is an example of redox as well as electrostatic switching.

Redox switching of surface properties has significant potential in cell biology as it affords the opportunity to conduct mechanistic studies of cell attachment and the dynamics of how changes to a surface influence cell structural organization and intracellular signaling. Such studies have important implications for biomaterial developments. A good example is the demonstration that switchable surfaces based on SAMs can be used in controlling cell migration [147]. This was achieved using SAMs, patterned by microcontact printing [148]. One set of locations in the SAM were terminated in methyl moieties ( $\text{HS}(\text{CH}_2)_{17}\text{CH}_3$ ) forming hydrophobic patches to which cells adsorb. These hydrophobic patches were surrounded by SAM-forming molecules terminated in oligo(ethylene glycol) ( $\text{HS}(\text{CH}_2)(\text{OCH}_2\text{OCH}_2)_3\text{OH}$ ) moieties that resist the adsorption of proteins and cells from solution. Having allowed the cells to attach on the hydrophobic regions, and spread to the limits of these regions, it is then possible to selectively remove the oligo(ethylene glycol) moieties instantly, so the cells can start to migrate across the surface. The switching is achieved by the

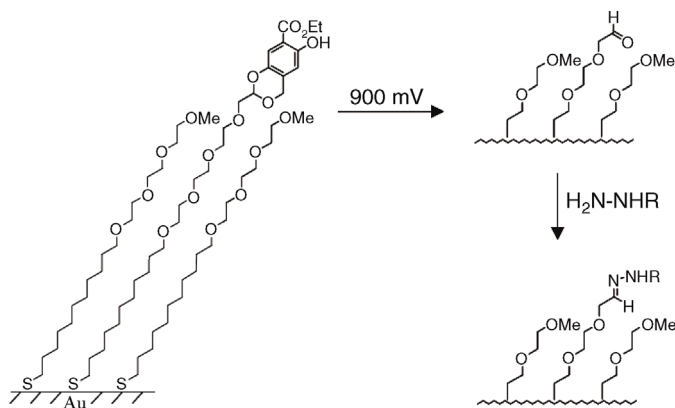


**Figure 1.28** Scheme using potential cleavable molecules to switch the surface chemistry. (Reprinted with permission from Ref. [149]. © 2004 Wiley-VCH Verlag GmbH & Co. KGaA.)

application of a brief voltage pulse to the gold electrode at a potential that removes only the oligo(ethylene glycol) moieties. This is possible due to the inferior chain packing of the oligo(ethylene glycol) moieties relative to the  $\text{HS}(\text{CH}_2)_{17}\text{CH}_3$ . The inferior packing means that there are fewer van der Waals interactions between the alkyl chains. Consequently, the SAMs in these regions are less stable on the surface and can therefore be preferentially removed. As soon as the oligo(ethylene glycol) moieties are removed from the surface, proteins from the culture medium adsorb onto the gold surface, and generate a surface where cells can spread across. The ability to grow cells in patterns, and then to release them from these patterns with a simple electrochemical manipulation, provides the basis for new types of bioassays that make use of observations of cell motility.

More advanced electrochemical manipulation of cells on surfaces can be achieved with custom-synthesized switchable molecules. Mrksich and coworkers recently [149] demonstrated a SAM on gold with a 4-*H*-benzo[*d*][1,3]dioxinol terminal group (Figure 1.28). Subjecting the monolayer to a potential of 900 mV versus Ag|AgCl caused the oxidation of the aromatic ring of the 4-*H*-benzo[*d*][1,3]dioxinol with hydrolysis of the acetal to yield the aldehyde. The resulting aldehyde can be used for ligand immobilization, with corresponding protein capture or, alternatively, the surface can be used for studies of cell migration. The latter is demonstrated in the paper where surfaces were patterned with circular islands of hexadecanethiols to which fibronectin was adsorbed such that cells would adhere. The rest of the surface was modified with a mixed SAM as depicted in Figure 1.28 where the 4-*H*-benzo[*d*][1,3]dioxinol-terminated species was only 2%. The fibroblast cells used did not spread in these regions and hence circular patterns of cells were observed. After 4 h of culturing the cells, a potential of 900 mV versus Ag|AgCl was applied to the monolayer for 10 s. The cells began to migrate from these regions and after 10 h the circular patterns of cells were no longer evident.

Mrksich and coworkers [150] demonstrated even more sophisticated switchable surfaces where cells could be sequentially released and reattached. A SAM that

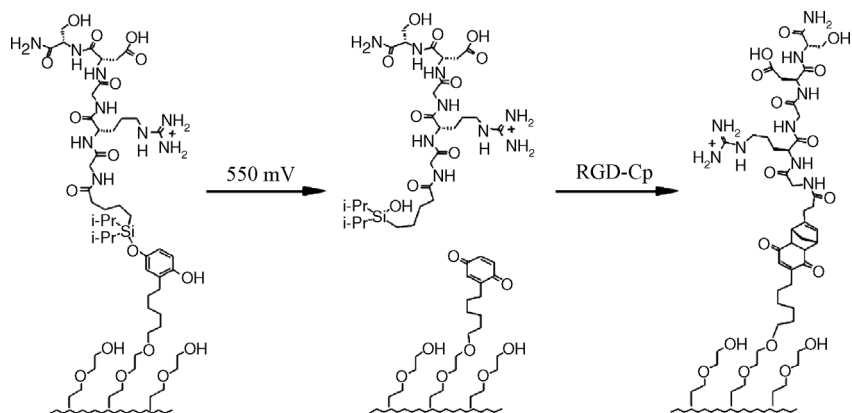


**Figure 1.29** Scheme of sophisticated switchable surfaces where cells could be sequentially released and reattached. A self-assembled monolayer, using an O-silyl hydroquinone as the cleavable molecule, allows for the release and reattachment of cells onto a surface. (Reprinted with permission from Ref. [150]. ©2003 American Chemical Society.)

incorporated an O-silyl hydroquinone moiety was employed (Figure 1.29). To the distal end of the molecules a peptide ligand, Arg-Gly-Asp (known as RGD peptide) was attached. RGD is a ligand for integrin receptors, molecules on the cell surface that mediate cell adhesion. The O-silyl hydroquinone ether is electroactive and allows for the selective release of the peptide from the substrate. The release is triggered by applying a potential to the substrate of 550 mV versus Ag|AgCl, which oxidizes the hydroquinone to the corresponding benzoquinone with hydrolysis of the silyl ether. The resulting benzoquinone group undergoes a selective immobilization reaction with a diene-tagged peptide by way of a Diels–Alder reaction and therefore, provides the basis for a second dynamic event. The benzoquinone is redox active and can be reduced back to the hydroquinone, which prevents immobilization of the diene-tagged ligand. In this work, Yeo *et al.* demonstrated that surfaces could be switched from initially being adhesive to all cells, to release cells and then following addition of a new ligand to the surface, switching back to being adhesive to cells again.

These types of switchable electrode surfaces have been used to selectively pattern two different cell populations onto a surface [151] and additionally these surfaces can selectively release different cells at different applied potentials [152]. However, it is important to recognize that electrochemically switching a surface from inactive to conjugation and active to conjugation has been well explored with nitro-terminated aryl diazonium salts. In such studies, the application where very anodic potential resulted in a six-electron reduction to an amine [139], to which proteins could be attached [153–155]. The key difference is that the interaction of the biological medium with the surface is controlled by the presence of the antifouling layer. In many ways these electrode surfaces developed by Mrksich and coworkers [150–152, 156] are very similar to the antifouling surfaces with molecular wires discussed in Section 1.4.2 [131, 132, 138, 142]. In both cases the electrode is

effectively passivated by the presence of an antifouling layer and electrochemical communication is achieved via electron transfer through the organic monolayer to a redox-active species attached to its surface. The next step in the development of these electrodes could in fact be the combination of these two concepts, where surfaces show electrochemically switchable properties, which control the response of cells and at the same time the surface could act as a sensing surface and monitor changes in the cells biochemically.

### 1.5.2

#### Control and Enhancement of Electrochemical Reactions using Magnetic Nanostructures on Electrodes

The electrochemically switchable surfaces discussed rely on either a change in conformation of molecules attached to an electrode surface, or a change in the actual attached moieties, to give switchable properties. Recent advances in magnetic nanoparticles, and the modification of these particle surfaces, offers a range of unique opportunities to switch the properties of electrochemical systems by using magnetic fields to achieve spatial control over the position of the functionalized magnetic structures. The aim of spatially manipulating these magnetic structures by altering the magnetic field location or orientation is to allow for the systematic control of reactions on electrode surfaces.

This concept in the form of ‘magneto-switching’ was pioneered by Willner and coworkers [132, 157], who demonstrated the ability to reversibly switch ‘ON’ and ‘OFF’ bioelectrocatalytic reactions by changing the position of an applied magnetic field to provide vertical spatial control over magnetic particles. In this work, a gold electrode modified with glucose oxidase was switched ‘ON’ by magnetically attracting 1- $\mu\text{m}$  magnetite particles modified with *N*-(ferrocenylmethyl) aminohexanoic acid mediators to the electrode that enabled the mediation of the enzyme reaction. The application of a potential of  $E^{\circ} = 0.31$  V vs. SCE caused the oxidation of the ferrocene to ferricinium ions, whereupon the ferricinium could oxidize the reduced glucose oxidase back to the catalytically active oxidized form [158]. (Figure 1.30a). The electrode was switched

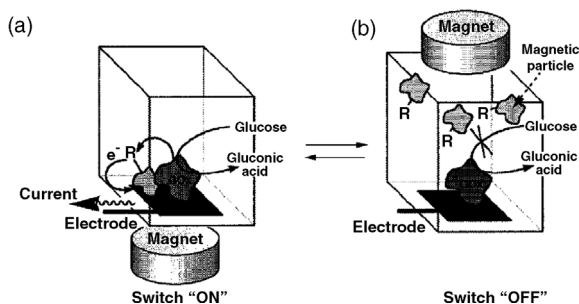


**Figure 1.30** Magneto-switched bioelectrocatalyzed oxidation of glucose in the presence of relay-functionalized magnetic particles. (Reprinted with permission from Ref. [157]. ©2000 American Chemical Society.)

'OFF' by repositioning the magnet on top of the cell. This drew the ferrocene-modified magnetite particles away the electrode such that no ferricinium was produced and hence prevented the mediation of the enzyme reaction by the mediator-modified nanoparticles (Figure 1.30b). In the same paper, the concept of magneto-switching was also applied to the reduction of  $\text{NO}_3^-$  using N-methyl-N'-(dodecanoic acid)-4,4'-bipyridinium as the redox mediator in the presence of nitrate reductase.

Willner and colleagues [159] extended this idea further to demonstrate lateral spatial control of magnetic particles that enabled the magneto-switching of the electrochemical generation of light. In this work, aminonaphthoquinone-modified magnetite particles were introduced into an electrochemical cell that consisted of a glass slide, half of which was plated with gold, to give a working electrode with the other half being nonconducting glass. As before, the electrode reaction was switched 'ON' by positioning a magnet under the gold electrode, which attracted the magnetite particles onto the electrode. This initiated the electrochemical reduction of naphthoquinone under oxygen [160] at the applied potential region  $E < -0.36\text{ V}$  to produce electrogenerated  $\text{H}_2\text{O}_2$ . The  $\text{H}_2\text{O}_2$  subsequently reacted with luminol in the presence of horseradish peroxidase to generate 3-amino-phthalate and light, ( $\lambda_{\text{em}} = 425\text{ nm}$ ) (Figure 1.31a). The lateral repositioning of the magnetic particles onto the nonconducting glass plate was achieved by moving the magnet. This switched 'OFF' the electrochemical quinone reduction and hence the light emission (Figure 1.31B). This novel demonstration revealed the potential use of such systems as logic 'AND' gated elements where light emission occurs only in the presence of a magnetic field and with an appropriate potential step applied to the electrode.

Wang and coworkers [161] have extended the magneto-switching concept by demonstrating a number of switchable electrochemical reactions using biomolecules, metallic nanoparticles [162] or functionalized magnetic particles. In the case of biomolecule modification, Wang and Kawde [161] attached DNA oligonucleotides onto streptavidin-coated magnetic particles. They demonstrated that by magnetically attracting the DNA-modified particles onto a gold electrode and by applying a constant anodic current of  $+5\ \mu\text{A}$  over a potential range of 0.6 to 1.2 V, a chronopotentiometric response corresponding to the oxidation of the guanine moiety ( $E_p = 1.02\text{ V}$ ) was observed. The electrochemical reaction was

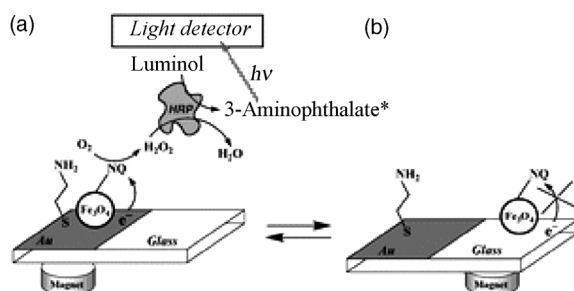


**Figure 1.31** Magneto-triggered biochemiluminescence. (Reproduced by permission of The Royal Society of Chemistry from [159].)

switched 'OFF' by magnetically removing the DNA-modified particles. They also demonstrated lateral spatial control of the particles by moving particles between two electrodes placed side-by-side and showed the corresponding switching of chronopotentiometric signals. In this way it is possible to envisage applications where separate electrochemical reactions on the same particles are sequentially monitored at different electrodes. Wang and coworkers [162] also demonstrated the use of Pt/Ru-functionalized nickel particles for the magneto-triggered electrochemical oxidation of methanol and the reduction of oxygen. They showed the switchability of this system through the reversible appearance and disappearance of voltammetric peak currents on the cyclic voltammograms, corresponding to the placement and removal of modified nickel nanoparticles, with no apparent carry over. The switchable control was shown to facilitate the on-demand switching of direct-methanol fuel cells. Musameh and Wang [163] also extended the concept of magneto-switching to carbon nanotubes (CNTs) where they took advantage of the magnetic and catalytic properties of CNTs without the need for functionalized magnetic nanoparticles.

Willner and coworkers [164] further advanced the utility of magneto-switching by demonstrating the dual quantification of two substrates within a sample. In this work, a gold-coated glass electrode was modified with ferrocene, while magnetic particles were modified with the electron mediator pyrroloquinoline quinone (PQQ) and the cofactor aminoethyl-functionalized-NAD<sup>+</sup> (aNAD<sup>+</sup>) as shown in Figure 1.32. Selective quantification of two substrates, glucose and lactate was reversibly accomplished by limiting the potential to a range that was appropriate to activate only one bioelectrocatalytic process. This idea exploits the difference in redox potentials of PQQ and ferrocene. In the case of lactate detection, this is switched on magnetically by bringing the nanoparticles with the cofactor for lactate (NAD<sup>+</sup>) into contact with the electrode. A potential range of  $-0.36\text{ V}$  to  $+0.15\text{ V}$  was

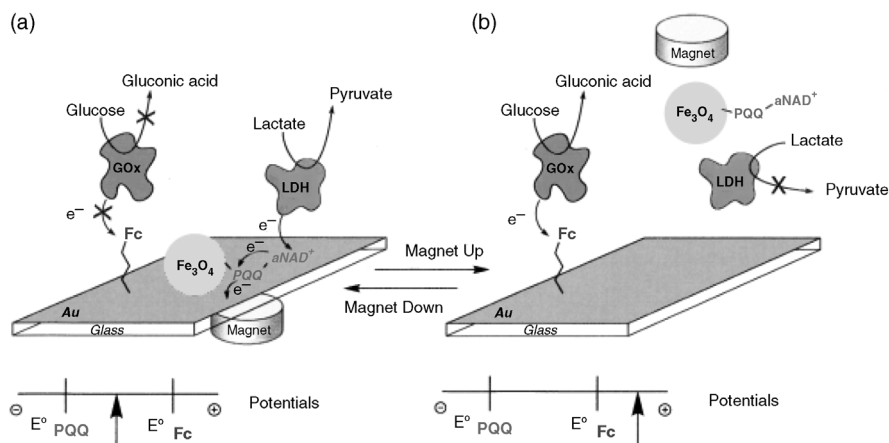


**Figure 1.32** Magneto-switched dual biosensing of glucose and lactate. (Reprinted with permission from Ref. [164]. ©2002 Wiley-VCH Verlag GmbH & Co. KGaA.)

applied to oxidize PQQ that initiates electron hopping to the electrode when lactate reduces the  $\text{NAD}^+$  cofactor to NADH in the presence of enzyme lactate dehydrogenase (LDH). The NADH is oxidized by PQQ, which results in the formation of  $\text{PQQH}_2$  and the regeneration of  $\text{NAD}^+$  (Figure 1.32a). The electrochemical oxidation of  $\text{PQQH}_2$  results in the observation of an anodic current. Movement of the magnet to draw magnetic particles away from the electrode, lactate oxidation was blocked and the applied potential was set to allow for only the oxidation and resulting quantification of glucose in the system (Figure 1.32b). Similar to the first example, magneto-switching using ferrocene-modified magnetic nanoparticles are utilized to control the accessibility of mediators to the enzymes by movements of a magnet.

A further significant development in the field of magneto-switchable control over magnetic nanostructures on electrodes was the use of alkyl-chain-functionalized hydrophobic magnetic particles in a two-phase system to control and switch the hydrophobic or hydrophilic properties of the electrode surface [165]. This concept was unique because it allows for dual functions depending on how the concept is applied. The first function involves utilizing the hydrophobic magnetic nanoparticles for blocking of the electrode surface. The nanoparticles form a hydrophobic thin film on the surface that is not permeable for water-soluble components, thus blocking aqueous electrochemistry from occurring at the electrode. This was demonstrated by Willner and coworkers [165] who showed reversible magneto-switching of the electron transfer of ferrocene at gold electrodes corresponding to the attraction (off) and withdrawal (on) of hydrophobic nanoparticles to and from the electrode surface. The second function involves the altering of the electrochemical reaction occurring on the electrode surface from aqueous-type processes to an organic-phase-type electrochemistry enabling the electrochemical detection of substrates dissolved in organic solvents. Willner and coworkers [166] demonstrated this function by monitoring the cyclic voltammograms of the reduction of cumene hydroperoxide dissolved in toluene. In this work, cumene hydroperoxide together with hydrophobic undecanoate-capped magnetite particles were kept away from a microperoxidase-11 (MP)-modified gold electrode immersed in an aqueous environment (Figure 1.33a). Microperoxidase-11 had previously been found to act as an electrocatalyst for the reduction of organic peroxides in nonaqueous solutions [167]. Switching of the position of the applied magnetic field to below the electrode switched 'ON' the reaction by attracting the hydrophobic magnetic particles along with coadsorbed toluene to the electrode surface. In this way, cumene hydroperoxide dissolved in the toluene is also brought to the electrode surface, where it is reduced by microperoxidase-11 upon the application of a potential of  $E^\circ = -0.7\text{ V}$  (Figure 1.33b).

Willner and coworkers [168] demonstrated the applicability of this method for a range of applications including the magneto-switching of DNA hybridization and polymerization for programmed DNA chips, of photocatalytically activated reactions using CdS nanoparticles for optobioelectronic systems [169], and of quinone oxidation and reduction for 'write-read-erase' information storage systems [170].

An exciting advancement of the magneto-switching concept involved the demonstration by Wang and coworkers [171] of the ability to use magnetic fields to control electrochemical reactivity on electrodes in comparison to previous demonstrations

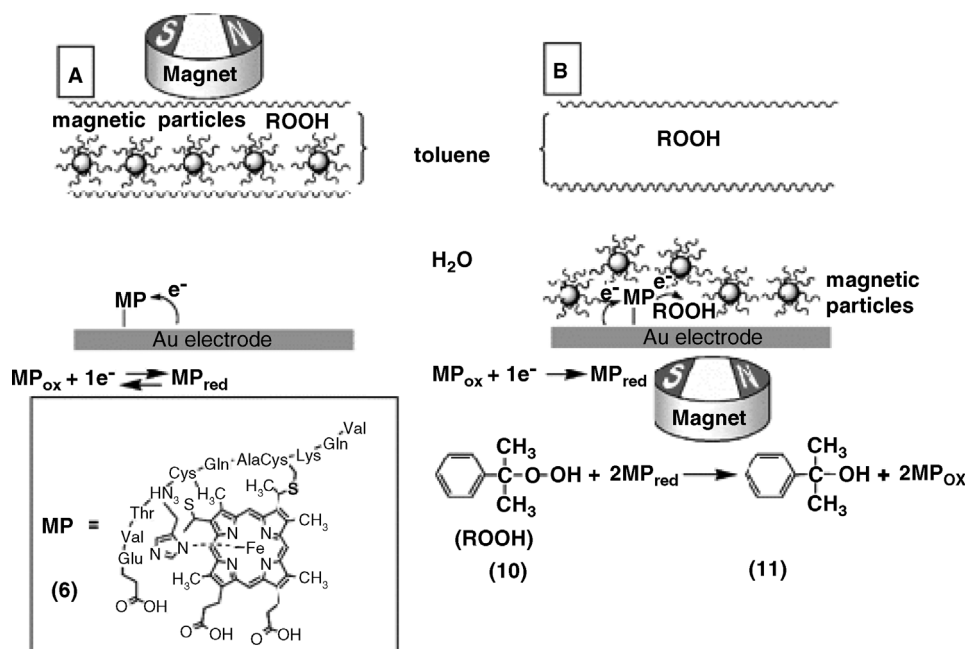


**Figure 1.33** Magneto-controlled ‘on/off’ switching of microperoxidase-11-catalyzed reduction of cumene hydroperoxide in an organic environment. (Reprinted with permission from Ref. [166]. ©2000 American Chemical Society.)

that were limited to ‘ON/OFF’ switching. This breakthrough introduced the unique ability of modulating electrocatalytic activity by orienting catalytic nickel nanowires on electrodes at different angles. In this work, 6- $\mu\text{m}$  nickel nanowires with diameters of 200 nm were synthesized via membrane template-directed electrodeposition for the oxidation of methanol and glucose. As nickel is known for its electrocatalytic action toward aliphatic alcohols, amino acids and carbohydrates [171], no further modification of the nanowires with mediators were required. Wang and coworkers demonstrated that electrochemical reactivity could be enhanced incrementally from a minimum when the nanowires were in the horizontal position on the carbon substrate (Figure 1.34a), to a maximum when the nanowires were in the vertical position (Figure 1.34b) by gradually changing the orientation of the applied magnetic field. This ability to tune electrode activity was attributed to changes in mass transport of glucose and methanol solutes due to tortuosity effects, as well as blocking effects that limit solute access to the portion of nickel surface facing the carbon electrodes.

The ability to selectively orientate nanowires on electrode surfaces was applied by Wang and coworkers [172] to provide on-demand protection for electrochemical sensors. In this study they showed that passivating the sensor electrode surfaces when measurements were not being taken could significantly increase the length of optimal performance of the sensor. Passivating the surface simply involved positioning of the magnetic field such that the alkanethiol-coated gold nanowires with a short

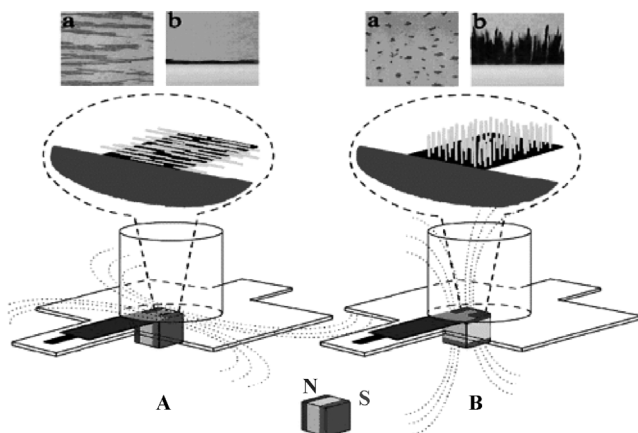


**Figure 1.34** Experimental setup showing the nickel nanowires in a (A) horizontal and (B) vertical position depending on the magnetic field orientation. (Reprinted with permission from Ref. [171]. ©2006 American Chemical Society.)

magnetic nickel segment were oriented in the horizontal position (Figure 1.35). This protects the electrode surface from fouling by blocking the access of surface-active materials between measurements. The ability of the nanowires to reversibly change the operation of the sensor in response to an external stimulus led the authors to describe them as ‘adaptive’. The same study also demonstrated that increasing both alkanethiol chain length and gold/nickel segment length ratio increased the

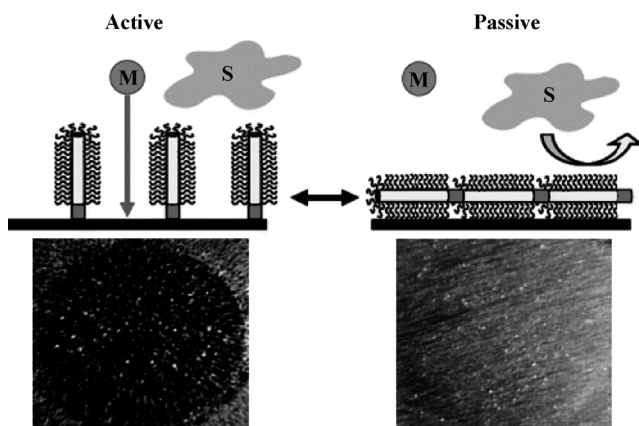


**Figure 1.35** On-demand protection of an electrochemical sensor. Trace analysis of metal (M) analyte in the presence of surface active compounds (S) using the ‘active’ and ‘passive’ states. (Reprinted with permission from Ref. [172]. ©2006 American Chemical Society.)

electrode-fouling resistance. Attractive sensor behavior was also demonstrated with stripping voltammograms showing well-defined concentration dependence for the detection of cadmium and significantly enhanced the length of optimal performance when the electrode was in the 'active' state compared with an unmodified gold electrode.

Further development of adaptive nanowires was carried out by Wang and coworkers [173] to extend the use of these magnetic structures for control of biocatalytic processes. In this example, the previously reported two-segment gold/nickel nanowires were functionalized with glucose oxidase (GOx) to provide control of biocatalytic oxidation of glucose in combination with a ferrocene mediator bound onto a gold-coated glass electrode. In this case, magnetic-field-controlled horizontal orientation of the GOx-modified nanowires allows effective contact between the enzyme and mediator, resulting in activation of the biocatalytic reaction. Vertical reorientation of the nanowires leads to reduced contact between the enzyme and the mediator resulting in reduced glucose oxidation. Importantly, this study demonstrated for the first time, complete withdrawal of the nanowires from the electrode surface that blocked activation of GOx, hence switching 'OFF' the reaction.

The ability to modulate electrochemical reactivity and effectively switch 'OFF' the reaction was extended further by Wang and coworkers [174] to control, on-demand, the separation and detection processes in microfluidic devices. In this work, the catalytic nickel nanowires were placed, reoriented and removed on-demand at the exit of the separation channel of the microfluidic chip, offering unique possibilities for controlling externally, events inside and outside a microchannel.

Recent work in the area of using magnetic structures on electrodes to control electrochemical reactions has centered primarily on the search for more effective materials used for the applications mentioned in this section to improve performance. An example of such work includes that of Vasilyev *et al.* [175] who attempted to improve the work of Willner and coworkers on logic gates by using very small ( $17 \pm 2$  nm) and monodispersed cobalt ferrite ( $\text{CoFe}_2\text{O}_4$ ) nanoparticles that are important for achieving the aim of reducing the error read-out possibility of logic gates. Similarly, Zhai *et al.* [176] extend the ideas of Wang and coworkers by utilizing nanowires made from the assembly of magnetic iron-oxide particles to show tunability of the oxidation of glucose by glucose oxidase. Another example is the work of Jimenez *et al.* [175] who used magnetic fields to self-assemble conductive nanowires consisting of Au-shell/ $\text{CoFe}_2\text{O}_4$  onto gold electrodes. In this work, these magnetic structures serve to increase the electrode surface area that results in up to a  $\sim 6.5$  fold enhancement in electrochemical response for the ferrocene-mediated oxidation of glucose by glucose oxidase when compared to an unmodified bare gold electrode.

It is clear that there remain many possibilities for extending the concept of using magnetic nanostructures on electrodes to control and enhance electrochemical reactions. It can be envisaged that the coming years should see the improvement of existing applications along with the exciting emergence of new applications utilizing the concepts highlighted in this section.

## 1.6

### Conclusions

Throughout this chapter we have described a range of different concepts from the literature where electrodes have been modified at the nanoscale to provide the electrode with unique capabilities. Throughout this chapter there has been emphasis on the properties relating to biological applications. In the simplest cases, this has been to increase the surface area for enhanced sensitivity or to provide electrocatalytic properties to the electrodes. However, nanostructuring electrodes have also enabled completely new concepts in electrochemistry to be explored, such as the interfacing of electrodes with proteins, having electrodes that are passivated from a sample solution such that electrochemical communication is only achieved through molecular wires, producing electrode surfaces with switchable properties or creating sensors where the spacing between conducting units is used to modulate the resistance of electrode layers.

Many of these unique properties are only possible because of the spatial control over the modification of the electrode and hence the emphasis throughout this chapter has been on control. However, our ability to structure electrodes at the nanoscale or even molecular level is really only in its infancy and so many new concepts will be revealed in the near future. To this point we have barely started considering vertically controlling the structure of electrodes at the molecular level and our ability to laterally structure electrodes with a high degree of control needs further development. With the latter in mind, a recent development by Buck and coworkers [177] is particularly important. In this work they showed, for the first time, strategies for patterning self-assembled monolayers using self-assembled supramolecular networks that are first assembled onto gold electrodes. What is unique about this work is that by placing electrodes modified with these networks into an alkanethiol solution for a short time enables the network to serve as a template for the alkanethiol deposition (that is the alkanethiol does not remove the network). In this way, patterns of alkanethiols can be produced, alternately copper patterning by this method was also demonstrated by the underpotential deposition of copper onto regions containing the alkanethiol but not the network. One cannot imagine what possibilities this new method of nanostructuring electrodes, nor many other new approaches, will bring, however, it is clear that developments will be rapid and exciting.

### References

- 1 Martin, C.R. and Foss, C.A. Jr (1996) *Laboratory Techniques in Electroanalytical Chemistry*.
- 2 Imisides, M.D., John, R., Riley, P.J. and Wallace, G.G. (1991) *Electroanalysis*, **3**, 879–889.
- 3 Wang, J. (1991) *Electroanalysis*, **3**, 255–259.
- 4 Malinauskas, A. (1999) *Synthetic Metals*, **107**, 75–83.
- 5 Situmorang, M., Gooding, J.J. and Hibbert, D.B. (1999) *Analytica Chimica Acta*, **394**, 211–223.

- 6 Markovic, N.M. and Ross, P.N. (2002) *Surface Science Reports*, **45**, 121–229.
- 7 Alexander, B.D., Kulesza, P.J., Rutkowska, L., Solarzka, R. and Augustynski, J. (2008) *Journal of Materials Chemistry*, **18**, 2298–2303.
- 8 Mathiyarasu, J., Pathak, S.S. and Yegnaraman, V. (2006) *Corrosion Reviews*, **24**, 307–321.
- 9 Adams, D.M., Brus, L., Chidsey, C.E.D., Creager, S., Creutz, C., Kagan, C.R., Kamat, P.V., Lieberman, M., Lindsay, S., Marcus, R.A., Metzger, R.M., Michel-Beyerle, M.E., Miller, J.R., Newton, M.D., Rolison, D.R., Sankey, O., Schanze, K.S., Yardley, J. and Zhu, X.Y. (2003) *The Journal of Physical Chemistry B*, **107**, 6668–6697.
- 10 Ybarra, G., Moyna, C., Florit, M.I. and Posadas, D. (2008) *Electrochimica Acta*, **53**, 3955–3959.
- 11 Haick, H. and Cahen, D. (2008) *Progress in Surface Science*, **83**, 217–261.
- 12 Mortimer, R.J. (1997) *Chemical Society Reviews*, **26**, 147–156.
- 13 Gooding, J.J., Mearns, F., Yang, W. and Liu, J. (2003) *Electroanalysis*, **15**, 81–96.
- 14 Love, J.C., Estroff, L.A., Kriebel, J.K., Nuzzo, R.G. and Whitesides, G.M. (2005) *Chemical Reviews*, **105**, 1103–1169.
- 15 Chen, D. and Li, J.H. (2006) *Surface Science Reports*, **61**, 445–463.
- 16 Cornell, B.A., Braach-Maksvytis, V.L.B., King, L.G., Osman, P.D.J., Raguse, B., Wieczorek, L. and Pace, R.J. (1997) *Nature*, **387**, 580–583.
- 17 Musick, M.D., Pena, D.J., Botsko, S.L., McEvoy, T.M., Richardson, J.N. and Natan, M.J. (1999) *Langmuir*, **15**, 844–850.
- 18 Patolsky, F., Gabriel, T. and Willner, I. (1999) *Journal of Electroanalytical Chemistry*, **479**, 69–73.
- 19 Freeman, R.G., Grabar, K.C., Allison, K.J., Bright, R.M., Davis, J.A., Guthrie, A.P., Hommer, M.B., Jackson, M.A., Smith, P.C., Walter, D.G. and Natan, M.J. (1995) *Science*, **267**, 1629–1632.
- 20 Blonder, R., Sheeney, L. and Willner, I. (1998) *Chemical Communications*, 1393–1394.
- 21 Liu, H., Tian, Y. and Xia, P. (2008) *Langmuir*, **24**, 6359–6366.
- 22 Terrill, R.H., Postlethwaite, T.A., Chen, C.-h., Poon, C.-D., Terzis, A., Chen, A., Hutchison, J.E., Clark, M.R., Wignall, G. et al. (1995) *Journal of the American Chemical Society*, **117**, 12537–12548.
- 23 Evans, S.D., Johnson, S.R., Cheng, Y.L. and Shen, T. (2000) *Journal of Materials Chemistry*, **10**, 183–188.
- 24 Krasteva, N., Besnard, I., Guse, B., Bauer, R.E., Muellen, K., Yasuda, A. and Vossmeier, T. (2002) *Nano Letters*, **2**, 551–555.
- 25 Katz, E., Willner, I. and Wang, J. (2004) *Electroanalysis*, **16**, 19–44.
- 26 Zamborini, F.P., Leopold, M.C., Hicks, J.F., Kulesza, P.J., Malik, M.A. and Murray, R.W. (2002) *Journal of the American Chemical Society*, **124**, 8958–8964.
- 27 Raguse, B., Chow, E., Barton, C.S. and Wieczorek, L. (2007) *Analytical Chemistry*, **79**, 7333–7339.
- 28 Velev, O.D. and Kaler, E.W. (1999) *Langmuir*, **15**, 3693–3698.
- 29 Park, S.J., Taton, T.A. and Mirkin, C.A. (2002) *Science*, **295**, 1503–1506.
- 30 Zheng, G., Patolsky, F., Cui, Y., Wang, W.U. and Lieber, C.M. (2005) *Nature Biotechnology*, **23**, 1294–1301.
- 31 Patolsky, F., Zheng, G., Hayden, O., Lakadamyali, M., Zhuang, X. and Lieber, C.M. (2004) *Proceedings of the National Academy of Sciences of the United States of America*, **101**, 14017–14022.
- 32 Piner, R.D., Zhu, J., Zu, F., Hong, S. and Mirkin, C.A. (1999) *Science*, **283**, 661–663.
- 33 Basnar, B., Weizmann, Y., Cheglakov, Z. and Willner, I. (2006) *Advanced Materials*, **18**, 713–718.
- 34 Zayats, M., Baron, R., Popov, I. and Willner, I. (2005) *Nano Letters*, **5**, 21–25.
- 35 Martin, C.R. (1994) *Science*, **266**, 1961–1966.
- 36 Hulteen, J.C. and Matrin, C.R. (1997) *Journal of Materials Chemistry*, **7**, 1075–1087.

- 37 Yamada, K., Gasparac, R. and Martin, C.R. (2004) *Journal of the Electrochemical Society*, **151**, E14–E19.
- 38 Huczko, A. (2000) *Applied Physics A*, **70**, 365–376.
- 39 Sides, C.R. and Martin, C.R. (2005) *Advanced Materials*, **17**, 125–128.
- 40 Li, N., Mitchell, D.T., Lee, Y.-P. and Martin, C.R. (2003) *Journal of the Electrochemical Society*, **150**, A979–A984.
- 41 Guo, Y.-G., Zhang, H.-M., Hu, J.-S., Wan, L.-J. and Bai, C.-L. (2005) *Thin Solid Films*, **484**, 341–345.
- 42 AlMawlawi, D., Coombs, N. and Moskovits, M. (1991) *Journal of Applied Physics*, **70**, 4421–4425.
- 43 Foss, C.A. Jr, Hornyak, G.L., Stockert, J.A. and Martin, C.R. (1992) *The Journal of Physical Chemistry*, **96**, 7497–7499.
- 44 Van-Dyke, L.S. and Martin, C.R. (1990) *Langmuir*, **6**, 1118–1123.
- 45 Cai, Z. and Martin, C.R. (1989) *Journal of the American Chemical Society*, **111**, 4138–4139.
- 46 Parthasarathy, R.V. and Martin, C.R. (1994) *Nature*, **369**, 298–301.
- 47 Sukeerthi, S. and Contractor, A.Q. (1999) *Analytical Chemistry*, **71**, 2231–2236.
- 48 Liang, W. and Martin, C.R. (1990) *Journal of the American Chemical Society*, **112**, 9666–9668.
- 49 Menon, V.P. and Martin, C.R. (1995) *Analytical Chemistry*, **67**, 1920–1928.
- 50 Brumlik, C.J. and Martin, C.R. (1991) *Journal of the American Chemical Society*, **113**, 3174–3175.
- 51 Brumlik, C.J., Menon, V.P. and Martin, C.R. (1994) *Journal of Materials Research*, **9**, 1174–1183.
- 52 Shin, C., Shin, W. and Hong, H.-G. (2007) *Electrochimica Acta*, **53**, 720–728.
- 53 Attard, G.S., Bartlett, P.N., Coleman, N.R.B., Elliott, J.M., Owen, J.R. and Wang, J.H. (1997) *Science*, **278**, 838–840.
- 54 Attard, G.S., Goltner, C.G., Corker, J.M., Henke, S. and Templer, R.H. (1997) *Angewandte Chemie-International Edition*, **36**, 1315–1317.
- 55 Bender, F., Chilcott, T.C., Coster, H.G.L., Hibbert, D.B. and Gooding, J.J. (2007) *Electrochimica Acta*, **52**, 2640–2648.
- 56 Imokawa, T., Williams, K.-J. and Denuault, G. (2006) *Analytical Chemistry*, **78**, 265–271.
- 57 Bender, F., Mankelov, R.K., Hibbert, D.B. and Gooding, J.J. (2006) *Electroanalysis*, **18**, 1558–1563.
- 58 Nelson, P.A., Elliott, J.M., Attard, G.S. and Owen, J.R. (2002) *Chemistry of Materials*, **14**, 524.
- 59 Whitehead, A.H., Elliott, J.M., Owen, J.R. and Attard, G.S. (1999) *Chemical Communications*, 331–332.
- 60 Bartlett, P.N., Birkin, P.N., Ghanem, M.A., De Groot, P. and Sawicki, M. (2001) *Journal of the Electrochemical Society*, **148**, C119–C123.
- 61 Evans, S.A.G., Elliott, J.M., Andrews, L.M., Bartlett, P.N., Doyle, P.J. and Denuault, G. (2002) *Analytical Chemistry*, **74**, 1322–1326.
- 62 Sun, F., Cai, W., Li, Y., Jia, L. and Lu, F. (2005) *Advanced Materials*, **17**, 2872–2877.
- 63 Huang, X., Meng, F., Pi, Z., Xu, W. and Liu, J. (2004) *Sensors and Actuators B*, **B99**, 444–450.
- 64 Shipway, A.N., Katz, E. and Willner, I. (2000) *ChemPhysChem*, **1**, 18–52.
- 65 Zhu, M., Liu, M., Shi, G., Xu, F., Ye, X., Chen, J., Jin, L. and Jin, J. (2002) *Analytica Chimica Acta*, **455**, 199–206.
- 66 Yu, A., Liang, Z., Cho, J. and Caruso, F. (2003) *Nano Letters*, **3**, 1203–1207.
- 67 Boennemann, H., Brinkmann, R. and Neiteler, P. (1994) *Applied Organometallic Chemistry*, **8**, 361–378.
- 68 Zhang, J., Kambayashi, M. and Oyama, M. (2004) *Electrochemistry Communications*, **6**, 683–688.
- 69 Zhang, J., Kambayashi, M. and Oyama, M. (2005) *Electroanalysis*, **17**, 408–416.
- 70 Li, J. and Lin, X.-Q. (2007) *Analytica Chimica Acta*, **596**, 222–230.
- 71 Manesh, K.M., Santhosh, P., Gopalan, A. and Lee, K.P. (2008) *Talanta*, **75**, 1307–1314.

- 72 Lu, Y., Yang, M., Qu, F., Shen, G. and Yu, R. (2007) *Bioelectrochemistry (Amsterdam, Netherlands)*, **71**, 211–216.
- 73 Selvaraju, T. and Ramaraj, R. (2005) *Journal of Electroanalytical Chemistry*, **585**, 290–300.
- 74 Wang, S., Yin, Y. and Lin, X. (2004) *Electrochemistry Communications*, **6**, 259–262.
- 75 Wang, H., Huang, Y., Tan, Z. and Hu, X. (2004) *Analytica Chimica Acta*, **526**, 13–17.
- 76 Chaki, N.K. and Vijaymohan, K. (2002) *Biosensors & Bioelectronics*, **17**, 1–12.
- 77 Gooding, J.J. and Hibbert, D.B. (1999) *Trends in Analytical Chemistry*, **18**, 525–533.
- 78 Willner, I. (2002) *Science*, **298**, 2407–2408.
- 79 Hall, E.A.H., Gooding, J.J. and Hall, C.E. (1995) *Mikrochimica Acta*, **121**, 119–145.
- 80 Ruzgas, T., Csoregi, E., Emneus, J., Gorton, L. and Marko-Varga, G. (1996) *Analytica Chimica Acta*, **330**, 123–138.
- 81 Varfolomeev, S.D., Kurochkin, I.N. and Yaropolov, A.I. (1996) *Biosensors & Bioelectronics*, **11**, 863–871.
- 82 Liu, S.Q., Leech, D. and Ju, H.X. (2003) *Analytical Letters*, **36**, 1–19.
- 83 Chen, D., Wang, G. and Li, J.H. (2007) *Journal of Physical Chemistry C*, **111**, 2351–2367.
- 84 Heller, A. (1990) *Accounts of Chemical Research*, **23**, 128–134.
- 85 Hecht, H.J., Schomburg, D., Kalisz, H. and Schmid, R.D. (1993) *Biosensors & Bioelectronics*, **8**, 197–203.
- 86 Liu, J., Paddon-Row, M.N. and Gooding, J.J. (2004) *The Journal of Physical Chemistry B*, **108**, 8460–8466.
- 87 Xiao, Y., Patolsky, F., Katz, E., Hainfeld, J.F. and Willner, I. (2003) *Science*, **299**, 1877–1881.
- 88 Holmlin, R.E., Ismagilov, R.F., Haag, R., Mujica, V., Ratner, M.A., Rampi, M.A. and Whitesides, G.M. (2001) *Angewandte Chemie-International Edition*, **40**, 2316.
- 89 Brown, K.R., Fox, A.P. and Natan, M.J. (1996) *Journal of the American Chemical Society*, **118**, 1154–1157.
- 90 Liu, T., Zhong, J., Gan, X., Fan, C.H., Li, G.X. and Matsuda, N. (2003) *ChemPhysChem*, **4**, 1364–1366.
- 91 Jensen, P.S., Chi, Q., Grummen, F.B., Abad, J.M., Horsewell, A., Schiffrin, D.J. and Ulstrup, J. (2007) *Journal of Physical Chemistry C*, **111**, 6124–6132.
- 92 Guiseppi-Elie, A., Lei, C.H. and Baughman F.R.H. (2002) *Nanotechnology*, **13**, 559–564.
- 93 Jiang, L., McNeil, C.J. and Cooper, J.M. (1995) *Journal of the Chemical Society. Chemical Communications*, 1293–1295.
- 94 Gooding, J.J. (2005) *Electrochimica Acta*, **50**, 3049–3060.
- 95 Zhao, Y.D., Zhang, W.D., Chen, H. and Luo, Q.M. (2002) *Analytical Sciences*, **18**, 939–941.
- 96 Chou, A., Bocking, T., Singh, N.K. and Gooding, J.J. (2005) *Chemical Communications*, 842–844.
- 97 Gooding, J.J., Chou, A., Liu, J.Q., Losic, D., Shapter, J.G. and Hibbert, D.B. (2007) *Electrochemistry Communications*, **9**, 1677–1683.
- 98 Gao, M., Huang, S.M., Dai, L.M., Wallace, G., Gao, R.P. and Wang, Z.L. (2000) *Angewandte Chemie-International Edition*, **39**, 3664–3667.
- 99 Gao, M., Dai, L.M. and Wallace, G.G. (2003) *Electroanalysis*, **15**, 1089–1094.
- 100 Yang, Y.Y., Huang, S.M., He, H., Mau, A.W.H. and Dai, L.M. (1999) *Journal of the American Chemical Society*, **121**, 10832–10833.
- 101 Li, J., Cassell, A., Delzeit, L., Han, J. and Meyyappan, M. (2002) *The Journal of Physical Chemistry B*, **106**, 9299–9305.
- 102 Koehne, J., Chen, H., Li, J., Cassell, A.M., Ye, Q., Ng, H.T., Han, J. and Meyyappan, M. (2003) *Nanotechnology*, **14**, 12391245.
- 103 Koehne, J., Li, J., Cassell, A.M., Chen, H., Ye, Q., Ng, H.T., Han, J. and Meyyappan, M. (2004) *Journal of Materials Chemistry*, **14**, 676–684.
- 104 Zhang, Y.G., Chang, A.L., Cao, J., Wang, Q., Kim, W., Li, Y.M., Morris, N., Yenilmez, E., Kong, J. and Dai, H.J. (2001) *Applied Physics Letters*, **79**, 3155–3157.

- 105 Liu, Z.F., Shen, Z.Y., Zhu, T., Hou, S.F., Ying, L.Z., Shi, Z.J. and Gu, Z.N. (2000) *Langmuir*, **16**, 3569–3573.
- 106 Yu, X.F., Mu, T., Huang, H.Z., Liu, Z.F. and Wu, N.Z. (2000) *Surface Science*, **461**, 199–207.
- 107 Diao, P., Liu, Z.F., Wu, B., Nan, X., Zhang, J. and Wei, Z. (2002) *ChemPhysChem*, **3**, 898–901.
- 108 Gooding, J.J., Rahmat, W., Liu, J.Q., Yang, W.R., Losic, D., Orbons, S., Mearns, F.J., Shapter, J.G. and Hibbert, D.B. (2003) *Journal of the American Chemical Society*, **125**, 9006–9007.
- 109 Yu, X., Chattopadhyay, D., Galeska, I., Papadimitrakopoulos, F. and Rusling, J.F. (2003) *Electrochemistry Communications*, **5**, 408–411.
- 110 Patolsky, F., Weizmann, Y. and Willner, I. (2004) *Angewandte Chemie-International Edition*, **43**, 2113–2117.
- 111 Yu, J.X., Shapter, J.G., Johnston, M.R., Quinton, J.S. and Gooding, J.J. (2007) *Electrochimica Acta*, **52**, 6206–6211.
- 112 Yu, J.X., Losic, D., Marshall, M., Bocking, T., Gooding, J.J. and Shapter, J.G. (2006) *Soft Matter*, **2**, 1081–1088.
- 113 Liu, J.Q., Chou, A., Rahmat, W., Paddon-Row, M.N. and Gooding, J.J. (2005) *Electroanalysis*, **17**, 38–46.
- 114 Willner, I., Heleg-Shabtai, V., Blonder, R., Katz, E. and Tao, G.L. (1996) *Journal of the American Chemical Society*, **118**, 10321–10322.
- 115 Katz, E., Riklin, A., Heleg-Shabtai, V., Willner, I. and Bückmann, A.F. (1999) *Analytica Chimica Acta*, **385**, 45–58.
- 116 Zayats, M., Katz, E. and Willner, I. (2002) *Journal of the American Chemical Society*, **124**, 2120–2121.
- 117 Zayats, M., Katz, E. and Willner, I. (2002) *Journal of the American Chemical Society*, **124**, 14724–14735.
- 118 Hess, C.R., Juda, G.A., Dooley, D.M., Amii, R.N., Hill, M.G., Winkler, J.R. and Gray, H.B. (2003) *Journal of the American Chemical Society*, **125**, 7156–7157.
- 119 Contakes, S.M., Juda, G.A., Langley, D.B., Halpern-Manners, N.W., Duff, A.P., Dunn, A.R., Gray, H.B., Dooley, D.M., Guss, J.M. and Freeman, H.C. (2005) *Proceedings of the National Academy of Sciences of the United States of America*, **102**, 13451–13456.
- 120 Langley, D.B., Brown, D.E., Cheruzel, L.E., Contakes, S.M., Duff, A.P., Hilmer, K.M., Dooley, D.M., Gray, H.B., Guss, J.M. and Freeman, H.C. (2008) *Journal of the American Chemical Society*, **130**, 8069–8078.
- 121 Sikes, H.D., Smalley, J.F., Dudek, S.P., Cook, A.R., Newton, M.D., Chidsey, C.E.D. and Feldberg, S.W. (2001) *Science*, **291**, 1519–1523.
- 122 Creager, S., Yu, C.J., Bamdad, C., O'Connor, S., MacLean, T., Lam, E., Chong, Y., Olsen, G.T., Luo, J., Gozin, M. and Kayem, J.F. (1999) *Journal of the American Chemical Society*, **121**, 1059–1064.
- 123 Wei, J.J., Liu, H.Y., Khoshtariya, D.E., Yamamoto, H., Dick, A. and Waldeck, D.H. (2002) *Angewandte Chemie-International Edition*, **41**, 4700–4703.
- 124 Wei, J.J., Liu, H.Y., Niki, K., Margoliash, E. and Waldeck, D.H. (2004) *The Journal of Physical Chemistry B*, **108**, 16912–16917.
- 125 Wei, J.J., Liu, H.Y., Dick, A.R., Yamamoto, H., He, Y.F. and Waldeck, D.H. (2002) *Journal of the American Chemical Society*, **124**, 9591–9599.
- 126 Adenier, A., Cabet-Deliry, E., Lalot, T., Pinson, J. and Podvorica, F. (2002) *Chemistry of Materials*, **14**, 4576–4585.
- 127 Downard, A.J. (2000) *Electroanalysis*, **12**, 1085–1096.
- 128 Gooding, J.J. (2008) *Electroanalysis*, **20**, 573–582.
- 129 Blanford, C.F., Heath, R.S. and Armstrong, F.A. (2007) *Chemical Communications*, 1710–1712.
- 130 Sumner, J.J. and Creager, S.E. (2001) *The Journal of Physical Chemistry B*, **105**, 8739–8745.
- 131 Liu, G.Z. and Gooding, J.J. (2006) *Langmuir*, **22**, 7421–7430.
- 132 Liu, G.Z., Paddon-Row, M.N. and Gooding, J.J. (2007) *Electrochemistry Communications*, **9**, 2218–2223.

- 133 Liu, J., Gooding, J.J. and Paddon-Row, M.N. (2005) *Chemical Communications*, 631–633.
- 134 Liu, J.Q., Paddon-Row, M.N. and Gooding, J.J. (2006) *Chemical Physics*, **324**, 226–235.
- 135 Chi, Q., Zhang, J. and Dong, S.J. (1994) *Electrochimica Acta*, **39**, 2431–2438.
- 136 Bourdillon, C., Demaille, C., Gueris, J., Moiroux, J. and Saveant, J.-M. (1993) *Journal of the American Chemical Society*, **115**, 12264–12269.
- 137 Gooding, J.J., Erokhin, P., Losic, D., Yang, W.R., Policarpio, V., Liu, J.Q., Ho, F.M., Situmorang, M., Hibbert, D.B. and Shapter, J.G. (2001) *Analytical Sciences*, **17**, 3–9.
- 138 Umek, R.M., Lin, S.W., Vielmetter, J., Terbrueggen, R.H., Irvine, B., Yu, C.J., Kayyem, J.F., Yowanto, H., Blackburn, G.F., Farkas, D.H. and Chen, Y.P. (2001) *The Journal of Molecular Diagnostics*, **3**, 74–84.
- 139 Delamar, M., Hitmi, R., Pinson, J. and Saveant, J.M. (1992) *Journal of the American Chemical Society*, **114**, 5883–5884.
- 140 Liu, G.Z., Bocking, T. and Gooding, J.J. (2007) *Journal of Electroanalytical Chemistry*, **600**, 335–344.
- 141 Ligler, F.S. and Rowe Taitt, C.A. (2002) *Optical Biosensors: Present and Future*, Elsevier.
- 142 Liu, G., Paddon-Row, M.N. and Gooding, J.J. (2008) *Chemical Communications*, 3870–3872.
- 143 Lahann, J. and Langer, R. (2005) *MRS Bulletin*, **30**, 185–188.
- 144 Lahann, J., Mitrogotri, S., Tran, T.N., Kaido, H., Sundaram, J., Choi, I.S., Hoffer, S., Somorjai, G.A. and Langer, R. (2003) *Science*, **299**, 371–374.
- 145 Wang, X.M., Katz, E. and Willner, I. (2003) *Electrochemistry Communications*, **5**, 814–818.
- 146 Wang, X.M., Kharitonov, A.B., Katz, E. and Willner, I. (2003) *Chemical Communications*, 1542–1543.
- 147 Jiang, X.Y., Ferrigno, R., Mrksich, M. and Whitesides, G.M. (2003) *Journal of the American Chemical Society*, **125**, 2366–2367.
- 148 Xia, Y. and Whitesides, G.M. (1998) *Angewandte Chemie-International Edition*, **37**, 551–575.
- 149 Yeo, W.-S. and Mrksich, M. (2004) *Advanced Materials*, **16**, 1352–1356.
- 150 Yeo, W.S., Yousaf, M.N. and Mrksich, M. (2003) *Journal of the American Chemical Society*, **125**, 14994–14995.
- 151 Yousaf, M.N., Houseman, B.T. and Mrksich, M. (2001) *Proceedings of the National Academy of Sciences of the United States of America*, **98**, 5992–5996.
- 152 Yeo, W.S. and Mrksich, M. (2006) *Langmuir*, **22**, 10816–10820.
- 153 Wang, J. and Carlisle, J.A. (2006) *Diamond and Related Materials*, **15**, 279–284.
- 154 Zhou, Y.L. and Zhi, J.F. (2006) *Electrochemistry Communications*, **8**, 1811–1816.
- 155 Vakurov, A., Simpson, C.E., Daly, C.L., Gibson, T.D. and Millner, P.A. (2004) *Biosensors & Bioelectronics*, **20**, 1118–1125.
- 156 Yeo, W.S. and Mrksich, M. (2004) *Advanced Materials*, **16**, 1352.
- 157 Hirsch, R., Katz, E. and Willner, I. (2000) *Journal of the American Chemical Society*, **122**, 12053–12054.
- 158 Cass, A.E.G., Davis, G., Francis, G.D., Hill, H.A.O., Aston, W.J., Higgins, I.J., Plotkin, E.V., Scott, L.D.L. and Turner, A.P.F. (1984) *Analytical Chemistry*, **56**, 667–671.
- 159 Ichia, L.S.-H., Katz, E., Wasserman, J. and Willner, I. (2002) *Chemical Communications*, 158–159.
- 160 Calabrese, G.S., Buchanan, R.M. and Wrighton, M.S. (1983) *Journal of the American Chemical Society*, **105**, 5594–5600.
- 161 Wang, J. and Kawde, A.-N. (2002) *Electrochemistry Communications*, **4**, 349–352.
- 162 Wang, J., Musameh, M., Laocharoensuk, R., González-García, O., Oni, J. and Gervasio, D. (2006) *Electrochemistry Communications*, **8**, 1106–1110.
- 163 Musameh, M. and Wang, J. (2005) *Langmuir*, **21**, 8565–8568.

- 164 Katz, E., Sheeney-Haj-Ichia, L., Bückmann, A.F. and Willner, I. (2002) *Angewandte Chemie-International Edition*, **41**, 1343–1346.
- 165 Katz, E., Sheeney-Haj-Ichia, L., Basnar, B., Felner, I. and Willner, I. (2004) *Langmuir*, **20**, 9714–9719.
- 166 Katz, E., Baron, R. and Willner, I. (2005) *Journal of the American Chemical Society*, **127**, 4060–4070.
- 167 Moore, A.N.J., Katz, E. and Willner, I. (1996) *Journal of Electroanalytical Chemistry*, **417**, 189–192.
- 168 Katz, E., Weizmann, Y. and Willner, I. (2005) *Journal of the American Chemical Society*, **127**, 9191–9200.
- 169 Katz, E. and Willner, I. (2005) *Angewandte Chemie-International Edition*, **44**, 4791–4794.
- 170 Katz, E. and Willner, I. (2006) *Electrochemistry Communications*, **8**, 879–882.
- 171 Wang, J., Scampicchio, M., Laocharoensuk, R., Valentini, F., Gonzalez-Garcia, O. and Burdick, J. (2006) *Journal of the American Chemical Society*, **128**, 4562–4563.
- 172 Laocharoensuk, R., Bulbarelo, A., Hocevar, S.B., Mannino, S., Ogorevc, B. and Wang, J. (2007) *Journal of the American Chemical Society*, **129**, 7774–7775.
- 173 Loaiza, Óscar A., Laocharoensuk, R., Burdick, J., Rodríguez, Marcella C., Pingarron, Jose M., Pedrero, M. and Wang, J. (2007) *Angewandte Chemie-International Edition*, **46**, 1508–1511.
- 174 Piccin, E., Laocharoensuk, R., Burdick, J., Carrilho, E. and Wang, J. (2007) *Analytical Chemistry*, **79**, 4720–4723.
- 175 Jimenez, J., Sheparovych, R., Pita, M., Narvaez Garcia, A., Dominguez, E., Minko, S. and Katz, E. (2008) *The Journal of Physical Chemistry C*, **112**, 7337–7344.
- 176 Zhai, Y., Zhai, J., Wen, D., Zhou, M., Zhang, L. and Dong, S. (2008) *Electrochemistry Communications*, **10**, 1172–1175.
- 177 Madueno, R., Raisanen Minna, T., Silien, C. and Buck, M. (2008) *Nature*, **454**, 618–621.